THE UNIVERSITY OF ALBERTA

LAMINAR FREE CONVECTION FROM A LARGE HORIZONTAL SURFACE

by

GERALD A. GLATZ, B.Sc. (Alberta)

A THESIS

SUBMITTED TO THE FACULTY OF GRADUATE STUDIES

IN PARTIAL FULFILMENT OF THE REQUIREMENTS FOR THE DEGREE

OF MASTER OF SCIENCE

DEPARTMENT OF MECHANICAL ENGINEERING

EDMONTON, ALBERTA

April 1966

UNIVERSITY OF ALBERTA

FACULTY OF GRADUATE STUDIES

The undersigned certify that they have read, and recommend to the Faculty of Graduate Studies for acceptance, a thesis entitled "LAMINAR FREE CONVECTION FROM A LARGE HORIZONTAL SURFACE" submitted by GERALD A. GLATZ in partial fulfilment of the requirements for the degree of Master of Science.

ABSTRACT

A theoretical and experimental investigation is presented for unsteady free convection adjacent to a heated horizontal plate subject to temporal variations of the surface temperature gradient. The equations of motion describing the flow near the surface were demonstrated to be of a linear nature provided inertia and advective effects could be neglected. On the basis of tests conducted in water, glycerine and air these approximations appear to be valid over a wide range of Prandtl numbers.

ACKNOWLEDGEMENTS

The author wishes to extend his appreciation to

- Dr. G.S.H. LOCK for his supervision of this thesis.
- the members of the Mechanical Engineering shop, particularly Mr. H. Golls who built the apparatus and Ray Marak who aided in the instrumentation.
- Lynne Fiveland for her patience in typing this thesis.
- the National Research Council for financial support under grant no. A-1672.

TABLE OF CONTENTS PAGE

PAGE

LIST OF ILLUSTRATIONS

NOMENCLATURE

x, X	distance parallel to surface
y, Y	distance normal to surface
u, U	velocity in X direction
v, V	velocity in Y direction
F, ψ	stream function
τ, t	time
p, P, Q	pressure
P°	hydrostatic pressure
P_d	pressure due to viscous or thermal effects
Φ, ϕ, θ	temperature
ν	momentum diffusivity
κ	thermal diffusivity
β	thermal expansion coefficient
ρ	density
c_p	specific heat at constant pressure
g	gravitational acceleration
μ	absolute viscosity
σ	Prandtl number
Os	Ostrach number
G	body force per unit mass
H	dissipation function
c	constant with dimension of (temperature)/(distance) $(\text{time})^n$

n	surface temperature index
ϵ, ζ, ξ	unknown functions
α, λ	arbitrary constants
γ_2	$-\alpha_4/2\ \alpha_1 = n$
ω, γ	roots of indicial equations
b	coefficient in Maclaurin expansion
z	arbitrary function
Γ	gamma function
$i^m\text{erfc}$	m'th integral of the complementary error function
s	Laplace transform variable
Δ	finite change
∇	Laplacian operator
η	$y/\left(\frac{4\tau}{\sigma}\right)^{1/2}$
$'$	denotes differentiation with respect to η

SUBSCRIPTS

d	departure
o	characteristic
w	surface
∞	infinity

Other symbols are defined where they appear.

CHAPTER I

INTRODUCTION

If a shallow horizontal layer of fluid is heated isothermally from below, there is no immediate visible motion of the fluid and, initially, heat is transferred from the lower region to the upper region by conduction alone. This can continue if the temperature differences in the fluid are small, but once a certain vertical temperature gradient is exceeded cellular motion occurs.* This problem of the motion of a fluid heated from below in a uniform body force field has been the subject of considerable study since the pioneering work of Lord Rayleigh (1)** in relation to experiments made by Benard (2) in 1900. He and many authors since then (3) have considered the problem as one of dynamic stability. The onset of instability is determined by a parameter, the Rayleigh number, which is independent of the cell shape.

Flow may also be established above and below heated isothermal surfaces by a thermal buoyancy effect (promoted by the existence of body forces) due to the presence of leading edges. These edges set up horizontal temperature

---

* It is interesting to note that a like cellular structure may be obtained in soapy water cooling from the surface.

** Numbers in brackets denote references given on page 67 .

gradients within the fluid which cause corresponding density gradients and hence pressure variations such that fluid flow results and a transfer of heat occurs. Stewartson (4) has analyzed the problem of steady, laminar, natural flow surrounding such isothermal plates by a similarity technique. A solution was obtained for heated plates facing downwards or cooled plates facing upwards, but in contrast, for heated plates facing upwards and cooled plates facing downwards a mathematical inconsistency was obtained due to an improperly posed problem. Levy (5) has tackled a similar problem using the Von Karman momentum integral method. Sugawara and Michiyochi (6) used an identical approach to calculate the distribution of the local heat transfer coefficient on both the upper and lower surfaces of a very thin ellipse. Their distribution agrees very well with the experimental work of Weise (7) who determined local heat transfer coefficients on rectangular plates in air. Weise was also the first to show that flow does exist on horizontal plates, by means of schlieren photography.

On a larger scale, in the field of micrometeorology, extensive theoretical and experimental work on horizontal surfaces has also been undertaken with specific reference to unsteady state conditions and turbulent flow. Some of the problems of interest have been the generation of mountain and valley winds (i.e. antitriptic winds) as analyzed by

Jeffreys (8) and the underlying principles of the sea breeze as considered by Pearce, Estoque and Fisher (9,10,11,12).

In the absence of a leading edge an isothermal surface could not generate flow. But if such a plate is heated differentially, the imposed temperature gradients again produce density gradients and hence pressure variations, resulting in motion adjacent to the surface. Here it is noticed that a uniform body force field is acting perpendicular to the surface but there is no particular restriction on heating or cooling or on whether the surface faces upwards or downwards. Assuming thermal (and hydrodynamic) stability, it is evident that laminar flow will exist if temperature gradients are moderate for either steady or nonsteady state conditions.

In the investigation to follow, the problem of laminar natural convection adjacent to a large horizontal surface is considered. In particular, the flow adjacent to a plate whose surface temperature gradient is a simple power law function of time is examined both theoretically and experimentally. The purpose of the thesis is: first, to determine temperature, pressure and velocity expressions describing the flow on surfaces without leading edges; second, to verify the validity of approximations made in the theoretical analysis (by performing experiments in water, glycerine and air).

CHAPTER II

THEORETICAL ANALYSIS

2.1 GOVERNING EQUATIONS

The problem of free convection from an infinitely large horizontal plate is considered. An attempt is made to reduce the Navier-Stokes equation and the corresponding energy equation to linear forms.

2.1-1 Formulation of Problem

Laminar incompressible flows due to heat conduction from a surface to a fluid in a uniform body force field are described by the following equations:

Mass:
$$\nabla \cdot \tilde{V} = 0 \quad *$$

Momentum:
$$\frac{D\tilde{V}}{Dt} = -\frac{1}{\rho}\nabla P + \tilde{G} + \nu\nabla^2\tilde{V} \qquad 2.1\text{-}1$$

Energy:
$$\frac{D\theta}{Dt} = \kappa\nabla^2\theta + \frac{\nu}{c_p} H$$

---

* Ignoring an extremely small contribution due to the material derivative.

Consider the application of these equations to the two-dimensional semi-infinite region illustrated in figure 2.1. If temperature changes are moderate, all properties except density may be taken as constant (13). The importance of a variable density is that it permits motion promoted

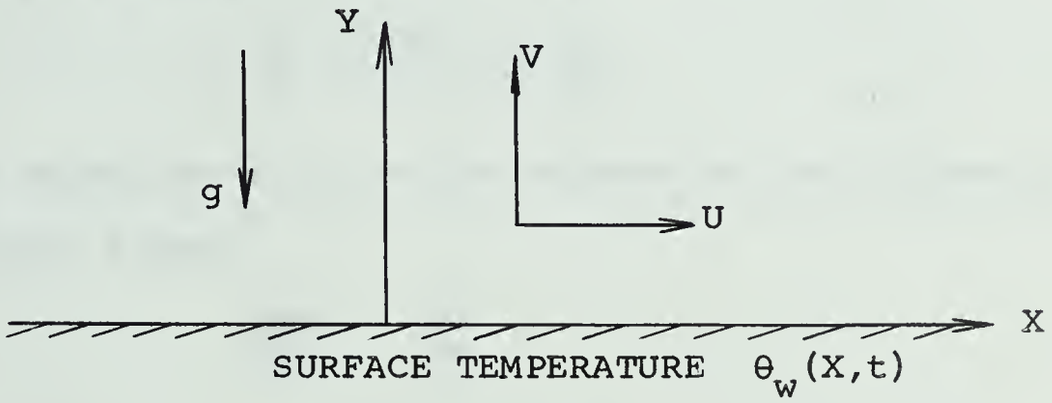

FIG. 2.1 COORDINATE SYSTEM

by buoyancy forces in the gravitational field of the earth. Density is taken as a function of temperature only, thereby permitting β, the coefficient of expansion, to be defined from the equation of state

$$\rho = \rho(\theta),$$

in accordance with the application of the Boussinesqian approximations

$$\frac{\rho}{\rho_\infty} \simeq 1 \qquad \text{and} \qquad \rho - \rho_\infty \neq 0.$$

Thermal radiation may be present but because most fluids have a low transmittance (except gases), its contribution is taken to be negligible.

Considering the surface temperature as a function of X and time, one would expect a boundary layer to form. The resulting change in pressure will be a departure from the hydrostatic pressure depending on whether the plate is heated or cooled. Taking

$$P = P^{o} + P_{d}$$

permits equations 2.1-1 to be reduced to the following two-dimensional forms:

$$\frac{\partial U}{\partial X} + \frac{\partial V}{\partial Y} = 0$$

$$\frac{\partial U}{\partial t} + U\frac{\partial U}{\partial X} + V\frac{\partial U}{\partial Y} = -\frac{1}{\rho}\frac{\partial P_d}{\partial X} + \nu\left(\frac{\partial^2 U}{\partial X^2} + \frac{\partial^2 U}{\partial Y^2}\right)$$

$$\frac{\partial V}{\partial t} + U\frac{\partial V}{\partial X} + V\frac{\partial V}{\partial Y} = -\frac{1}{\rho}\frac{\partial P_d}{\partial Y} + \beta g\theta + \nu\left(\frac{\partial^2 V}{\partial X^2} + \frac{\partial^2 V}{\partial Y^2}\right)$$

2.1-2

$$\frac{\partial \theta}{\partial t} + U\frac{\partial \theta}{\partial X} + V\frac{\partial \theta}{\partial Y} = \kappa\left(\frac{\partial^2 \theta}{\partial X^2} + \frac{\partial^2 \theta}{\partial Y^2}\right) +$$

$$\frac{2\nu}{c_p}\left[\left(\frac{\partial U}{\partial X}\right)^2 + \left(\frac{\partial V}{\partial Y}\right)^2\right] + \frac{\nu}{c_p}\left[\frac{\partial U}{\partial Y} + \frac{\partial V}{\partial X}\right]^2$$

Assuming no slip at the surface, and since flow does not occur outside the boundary layer, the problem is subject to the following initial and boundary conditions:

$$t = 0: \qquad (Y > 0) \qquad U = \theta = 0$$

$$Y = 0: \qquad (t > 0) \qquad U = 0,\ \theta = \theta_w\ (X,t)$$

$$Y = \infty: \qquad (t > 0) \qquad U = \theta = P_d = 0$$

2.1-3

2.1-2 Normalization of Equations

Traditional methods failed to normalize equations 2.1-2 for these required more than one known characteristic quantity. The only characteristic parameter available in this problem is the rate of change of surface temperature gradient with time (c). A procedure used by Hellums and Churchill (14) which defines characteristic quantities in terms of fluid properties does permit the normalization of equations 2.1-2.

If the dimensional quantities are written as

$$U = uU_o \quad , \quad V = vV_o \quad , \quad t = \tau t_o \quad , \quad X = xX_o \quad ,$$

$$Y = yY_o \quad , \quad P_d = pP_{do} \quad , \quad \text{and } \theta = \phi c t_o X_o^{*} \quad , \qquad 2.1\text{-}4$$

and substituted into equations 2.1-2, these equations then become

$$\frac{\partial u}{\partial x} + \left(\frac{X_o V_o}{Y_o U_o}\right) \frac{\partial v}{\partial y} = 0$$

---

* Taking n = 1 for simplicity.

$$\frac{\partial u}{\partial \tau} + \left(\frac{t_o U_o}{X_o}\right) u \frac{\partial u}{\partial x} + \left(\frac{t_o V_o}{Y_o}\right) v \frac{\partial u}{\partial y} = - \left(\frac{t_o P_{do}}{\rho U_o X_o}\right) \frac{\partial p}{\partial x}$$

$$+ \left(\frac{t_o \nu}{X_o^2}\right) \frac{\partial^2 u}{\partial x^2} + \left(\frac{t_o \nu}{Y_o^2}\right) \frac{\partial^2 u}{\partial y^2}$$

$$\frac{\partial v}{\partial \tau} + \left(\frac{t_o U_o}{X_o}\right) u \frac{\partial v}{\partial x} + \left(\frac{t_o V_o}{Y_o}\right) v \frac{\partial v}{\partial y} = - \left(\frac{t_o P_{do}}{\rho V_o Y_o}\right) \frac{\partial p}{\partial y}$$

2.1-5

$$+ \left(\frac{\beta g c t_o^2 X_o}{V_o}\right) \phi + \left(\frac{\nu t_o}{X_o^2}\right) \frac{\partial^2 v}{\partial x^2} + \left(\frac{t_o \nu}{Y_o^2}\right) \frac{\partial^2 v}{\partial y^2}$$

$$\frac{\partial \phi}{\partial \tau} + \left(\frac{U_o t_o}{X_o}\right) u \frac{\partial \phi}{\partial x} + \left(\frac{V_o t_o}{Y_o}\right) v \frac{\partial \phi}{\partial y} = \left(\frac{\kappa t_o}{X_o^2}\right) \frac{\partial^2 \phi}{\partial x^2} +$$

$$\left(\frac{\kappa t_o}{Y_o^2}\right) \frac{\partial^2 \phi}{\partial y^2} + 2 \left(\frac{\nu U_o^2}{c_p c x_o^3}\right) \left(\frac{\partial u}{\partial x}\right)^2 + 2 \left(\frac{\nu V_o^2}{c_p c X_o Y_o^2}\right) \left(\frac{\partial v}{\partial y}\right)^2$$

$$+ \left(\frac{\nu U_o^2}{c_p c X_o Y_o^2}\right) \left(\frac{\partial u}{\partial y}\right)^2 + 2 \left(\frac{\nu U_o V_o}{c_p c X_o^2 Y_o}\right) \left(\frac{\partial u}{\partial y} \frac{\partial v}{\partial x}\right) +$$

$$\left(\frac{\nu V_o^2}{c_p c X_o^3}\right) \left(\frac{\partial v}{\partial x}\right)^2 .$$

Assuming, for completeness, that all coefficients have the same order of magnitude, each group except $\kappa t_o / X_o^2$ and

$\kappa t_o/Y_o^2$ may be equated to unity. This will result in a system of algebraic equations, the solutions of which permit reference quantities to be defined in terms of fluid properties, and the characteristic quantity (c). $\kappa t_o/X_o^2$ and $\kappa t_o/Y_o^2$ are excluded because they combine with $\nu t_o/X_o^2$ and $\nu t_o/Y_o^2$ to give $\kappa/\nu = 1$ which contains no reference quantity. By not forcing these terms to unity, they appear as a dimensionless group (σ) in the boundary layer equations. Solving the above mentioned equations results in

$$X_o = Y_o = (\nu t_o)^{1/2} \quad , \qquad U_o = V_o = (\nu/t_o)^{1/2} \quad ,$$

$$P_{do} = \mu/t_o \quad , \qquad \text{and} \qquad t_o = (\beta g c)^{-1/3} \quad . \qquad \text{2.1-6}$$

Utilizing these definitions, it may be shown that the last five terms of the energy equations again combine into an expression which contains no reference quantity. Hence substituting 2.1-6 into 2.1-4 gives

$$x = \left(\frac{\beta g c}{\nu^3}\right)^{1/6} X, \quad y = \left(\frac{\beta g c}{\nu^3}\right)^{1/6} Y, \quad u = \frac{U}{(\beta g c \nu^3)^{1/6}} \quad ,$$

$$v = \frac{V}{(\beta g c \nu^3)^{1/6}} \quad , \quad \tau = (\beta g c)^{1/3} t, \quad p = \frac{P_d}{(\mu^3 \beta g c)^{1/3}}$$

$$\text{and} \quad \phi = \left(\frac{\beta g}{c \nu}\right)^{1/2} \theta \, .$$

As a consequence, the problem may be rephrased to one of obtaining a solution to the following normalized equations:

$$\frac{\partial u}{\partial x} + \frac{\partial v}{\partial y} = 0$$

$$\frac{\partial u}{\partial \tau} + u\frac{\partial u}{\partial x} + v\frac{\partial u}{\partial y} = -\frac{\partial p}{\partial x} + \frac{\partial^2 u}{\partial x^2} + \frac{\partial^2 u}{\partial y^2}$$

$$\frac{\partial v}{\partial \tau} + u\frac{\partial v}{\partial x} + v\frac{\partial v}{\partial y} = -\frac{\partial p}{\partial y} + \phi + \frac{\partial^2 v}{\partial x^2} + \frac{\partial^2 v}{\partial y^2}$$

2.1-7

$$\frac{\partial \phi}{\partial \tau} + u\frac{\partial \phi}{\partial x} + v\frac{\partial \phi}{\partial y} = \frac{1}{\sigma}\left(\frac{\partial^2 \phi}{\partial x^2} + \frac{\partial^2 \phi}{\partial y^2}\right)$$

$$+ \text{Os}\left[2\left(\frac{\partial u}{\partial x}\right)^2 + 2\left(\frac{\partial v}{\partial y}\right)^2 + \left(\frac{\partial u}{\partial y}\right)^2 + \left(\frac{\partial v}{\partial x}\right)^2 + 2\left(\frac{\partial u}{\partial y}\,\frac{\partial v}{\partial x}\right)\right]$$

where $\text{Os} = \dfrac{\nu^{1/2}(\beta g)^{5/6}}{c^{1/6}c_p} = \dfrac{\beta g X_o}{c_p}$ *.

Initial and boundary conditions now become :

---

* This ratio is analogous to the Eckert number in forced convection. It is suggested that it be called the Ostrach Number, Os.

$$\tau = 0: \qquad (y>0) \qquad u = \phi = 0$$

$$y = 0: \qquad (\tau>0) \qquad u = 0,\ \phi = \phi_w\ (x,\tau) \qquad 2.1\text{-}8$$

$$y = \infty: \qquad (\tau>0) \qquad u = \phi = p = 0$$

2.1-3 Order of Magnitude Analysis

It has been observed for boundary layer flows that

$$Y \ll X.$$

Since $X_o = Y_o$, it follows that

$$y \ll x,$$

and hence from the continuity equation 2.1-7

$$v \ll u.$$

Although an order of magnitude analysis may be made on the individual equations 2.1-7*, solutions of the combined momentum equation are considered in section 2.2. Therefore an analysis is made on that equation.

Eliminating pressure, the combined momentum equation becomes

$$\frac{\partial^2 u}{\partial y \partial \tau} - \frac{\partial^2 v}{\partial x \partial \tau} + u \frac{\partial^2 u}{\partial y \partial x} - u \frac{\partial^2 v}{\partial x^2} + v \frac{\partial^2 u}{\partial y^2} - v \frac{\partial^2 v}{\partial x \partial y}$$

---

* The result is the same as for the combined equations.

$$= \frac{\partial^3 u}{\partial y^3} + \frac{\partial^3 u}{\partial y \partial x^2} - \frac{\partial^3 v}{\partial x^3} - \frac{\partial^3 v}{\partial x \partial y^2} - \frac{\partial \phi}{\partial x} .$$

Replacing the derivatives by finite difference quotients, then substituting the approximate magnitude of v, the above equation may be reduced to

$$\frac{\partial^2 u}{\partial y \partial \tau} + u \frac{\partial^2 u}{\partial y \partial x} = \frac{\partial^3 u}{\partial y^3} + \frac{\partial^3 u}{\partial y \partial x^2} - \frac{\partial \phi}{\partial x} .$$

Since x is considered to be infinitely large, it follows from the continuity equation that

$$\frac{\partial u}{\partial x} = 0 \ ^* \qquad \text{and} \qquad \frac{\partial v}{\partial y} = 0 \ ^* ,$$

consequently this permits the combined momentum equation to be reduced to

$$\frac{\partial^2 u}{\partial y \partial \tau} = \frac{\partial^3 u}{\partial y^3} - \frac{\partial \phi}{\partial x} .$$

Now consider energy equation 2.1-7. Neglecting dissipation a priori, the equation becomes

$$\frac{\partial \phi}{\partial \tau} + u \frac{\partial \phi}{\partial x} + v \frac{\partial \phi}{\partial y} = \frac{1}{\sigma} \left(\frac{\partial^2 \phi}{\partial x^2} + \frac{\partial^2 \phi}{\partial y^2} \right) .$$

---

* Also justified on the grounds of a constant surface temperature gradient.

Again replacing the derivatives by finite difference quotients, then applying the above approximate magnitudes on v and x, it is evident that

$$\frac{\partial \phi}{\partial \tau} + u \frac{\partial \phi}{\partial x} = \frac{1}{\sigma} \left(\frac{\partial^2 \phi}{\partial y^2} \right) .$$

Assuming that the remaining advection term is negligible the boundary layer equations* become

$$\frac{\partial^2 u}{\partial y \partial \tau} = \frac{\partial^3 u}{\partial y^3} - \frac{\partial \phi}{\partial x} \qquad 2.1\text{-}9$$

$$\frac{\partial \phi}{\partial \tau} = \frac{1}{\sigma} \left(\frac{\partial^2 \phi}{\partial y^2} \right) .$$

2.1-4 Possible Similarity Solution

It will now be shown that a similarity solution exists (i.e. equations 2.1-9 may be reduced to a set of linear ordinary differential equations) for a large horizontal plate whose surface temperature gradient is a function of time only.

The continuity equation implies the existence of a dimensionless stream function $\psi = \psi(x,y,\tau)$ such that

---

* Justified a posteriori (see Appendix A).

$$u = \frac{\partial \psi}{\partial y} \qquad \text{and} \qquad v = -\frac{\partial \psi}{\partial x} .$$

Introducing a similarity variable

$$\eta(y,\tau) = y\epsilon(\tau)$$

and dependent variables

$$\psi(y,\tau) = \xi(\tau)\, F(\eta)$$

$$\Phi(x,y,\tau) = \zeta(x,\tau)\, \Phi(\eta)$$

in equations 2.1-9, we seek the unknown functions $\epsilon(\tau)$, $\xi(\tau)$ and $\zeta(x,\tau)$ such that the resulting equations transform to a system of ordinary differential equations in F and Φ. Substituting, gives

$$F^{IV} - \alpha_1 \eta\, F''' - \left[2\alpha_1 + \alpha_2\right] F'' - \alpha_3 \Phi = 0 \qquad 2.1\text{-}10$$

and $$\left(\frac{1}{\sigma}\right) \Phi'' - \alpha_1 \eta\, \Phi' - \alpha_4\, \Phi = 0 \qquad 2.1\text{-}11$$

where $$\alpha_1 = \left(\frac{1}{\epsilon^3}\right) \frac{\partial \epsilon}{\partial \tau} \qquad 2.1\text{-}12$$

$$\alpha_2 = \left(\frac{1}{\epsilon^2 \xi}\right) \frac{\partial \xi}{\partial \tau} \qquad 2.1\text{-}13$$

$$\alpha_3 = \left(\frac{1}{\epsilon^4 \xi}\right) \frac{\partial \zeta}{\partial x} \qquad 2.1\text{-}14$$

$$\alpha_4 = \left(\frac{1}{\epsilon^2 \zeta}\right) \frac{\partial \zeta}{\partial \tau} \qquad 2.1\text{-}15$$

Thus a similarity solution will exist provided it can be shown that all the coefficients α are constant.

It is obvious that there are more conditions available than unknowns, and therefore not all α's will be arbitrary. Proceeding then to the permissible forms of the unknowns, an elimination of ϵ between equations 2.1-12 and 2.1-13 results in the following ordinary differential equation which may be solved for ξ.

That is,

$$\frac{\gamma_1 - 1}{\gamma_1} \left(\frac{d\xi}{d\tau}\right)^2 = \xi \frac{d^2\xi}{d\tau^2} \qquad 2.1\text{-}16$$

where $$\gamma_1 = -\frac{\alpha_2}{2\alpha_1} .$$

The permissible solutions are:

$$\xi = (\lambda_1 \tau + \lambda_2)^{\gamma_1} \quad ; \text{ if } \frac{\gamma_1 - 1}{\gamma_1} \neq 1 \qquad 2.1\text{-}17a$$

$$\xi = \lambda_3 e^{\lambda_4 \tau} \quad ; \text{ if } \frac{\gamma_1 - 1}{\gamma_1} = 1 , \qquad 2.1\text{-}17b$$

noting that λ_1, λ_2, λ_3, and λ_4 are arbitrary constants. It is important to note that 2.1-17b is not a separate solution,

but merely the asymptote of 2.1-17a as $\gamma_1 \to \infty$.

Substituting back into 2.1-13 for ξ gives the permissible form of ϵ, namely

$$\epsilon \propto (\lambda_1 \tau + \lambda_2)^{-1/2} \quad .$$

If ζ is taken in the form of a product solution

$$\zeta(x,\tau) = M(x)\, N(\tau) \quad ,$$

an inspection of equations 2.1-14 and 2.1-15 reveals that

$$M(x) \propto x \quad .$$

Eliminating ϵ between 2.1-14 and 2.1-15, it can easily be shown that

$$N(\tau) = (\lambda_5 \tau + \lambda_6)^{\gamma_2} \quad ; \quad \text{if} \quad \frac{\gamma_2 - 1}{\gamma_2} \neq 1$$

$$N(\tau) = \lambda_7 e^{\lambda_8 \tau} \quad ; \quad \text{if} \quad \frac{\gamma_2 - 1}{\gamma_2} = 1$$

noting again that λ_5, λ_6, λ_7 and λ_8 are arbitrary constants.

In summary, a similarity solution does exist when the plate is very long and inertia and advection terms may be neglected. Knowing the permissible forms of the unknown functions ϵ, ξ and ζ and replacing γ_2 by n, it can be shown that

$$\eta = y/\left(\frac{4\tau}{\sigma}\right)^{1/2} \quad ,$$

$$\psi = \frac{16\tau^{n+2}}{\sigma} F(\eta) , \qquad (n \geqslant 0)$$

and $$\Phi = x\tau^{n} \Phi(\eta).$$

Hence the boundary layer equations become:

$$\sigma F^{IV} + 2\eta F''' - 4(n + 1) F'' - \Phi = 0 \qquad 2.1\text{-}18$$

$$\Phi'' + 2\eta \Phi' - 4n \Phi = 0 . \qquad 2.1\text{-}19$$

2.1-18 may be integrated once immediately. Satisfying the boundary condition on pressure gives

$$\sigma F''' + 2\eta F'' - 2(2n + 3) F' + \int_{\eta}^{\infty} \Phi \, d\eta = 0. \qquad 2.1\text{-}20$$

The remaining boundary conditions 2.1-8 transformed to the η domain are:

$$F(0) = F'(0) = \Phi'(0) - 1 = 0$$
$$F'(\infty) = \Phi(\infty) = 0 \qquad 2.1\text{-}21$$

2.2 SOLUTIONS TO THE BOUNDARY LAYER EQUATIONS

Solutions of 2.1-19 and 2.1-20 consistent with 2.1-21 may be found by initially solving for the temperature

distribution, then substituting and solving for the velocity distribution. Various mathematical techniques are available to determine these solutions: the method of Frobenius is used below and Laplace Transforms were utilized in Appendix B.

2.2-1 Series Solution For Temperature

Consider a solution of the energy equation

$$\Phi'' + 2\eta\,\Phi' - 4n\,\Phi = 0 \qquad 2.2\text{-}1$$

with boundary conditions $\Phi(0) = 1$, $\Phi(\infty) = 0$. Assuming this solution may take the form

$$\Phi(\eta) = \sum_{m=0}^{\infty} a_m\, \eta^{m+\omega}, \qquad (a_o \neq 0)$$

a recursion relation may be found by substituting and grouping coefficients of like powers of η, namely

$$a_r = \frac{-a_{r-2}\left[2(\omega + r - 2) - 4n\right]}{(\omega+r)\quad(\omega + r - 1)} .$$

The corresponding indicial equation is given by

$$a_o\,\omega\,(\omega - 1) = 0.$$

Considering the zero root, it is evident that a solution to equation 2.2-1 is

$$\Phi(\eta) = a_o \left[1 + 2n\eta^2 - \frac{2n}{3}(1 - n)\eta^4 + \frac{4n}{45}(1 - n)(2 - n)\eta^6 \ldots\right] \qquad 2.2\text{-}2$$

$$+ a_1\left[\eta - \frac{1}{3}(1 - 2n)\eta^3 + \frac{1}{30}(1 - 2n)(3 - 2n)\eta^5 - \frac{1}{630}(1 - 2n)(3 - 2n)(5 - 2n)\eta^7 \ldots\right].$$

The series solution corresponding to the root $\omega = 1$ is proportional to the second of the two infinite series obtained above. Consequently the solution for $\omega = 0$ which contains two arbitrary constants is taken as the complete primitive.

Satisfying the boundary condition $\Phi(0) = 1$ requires that $a_o = 1$. To obtain the sums of the individual series for large values of η, Euler's transformation may be used to improve the rate of convergence. Utilizing this transformation, the boundary condition at infinity requires that (15)

$$a_1 = -\frac{2\Gamma(n+1)}{\Gamma(n+1/2)}^{*}$$

A re-arrangement of the series in terms of Weber functions (15) permits the solution to be given as

$$\Phi(\eta) = 2^{2n}\,\Gamma(n+1)\,i^{2n}\mathrm{erfc}\,\eta, \qquad 2.2\text{-}3$$

where $2n = 0,1,2, \ldots\ldots$.

Plots for several values of n are illustrated on figure 2.2.

2.2-2 Series Solution For Pressure

Consider a solution of the momentum equation

$$\frac{\partial p}{\partial y} = \phi \qquad 2.2\text{-}4$$

with boundary condition $p(\infty) = 0$. Writing the pressure departure as

$$p(x,y,\tau) = x\tau^{n}\left(\frac{4\tau}{\sigma}\right)^{1/2} Q(\eta),$$

equation 2.2-4 may be written as

$$\frac{\partial Q}{\partial \eta} = \Phi(\eta) \qquad 2.2\text{-}5$$

---

* This result may also be found from the method of Laplace transforms as outlined in Appendix B.

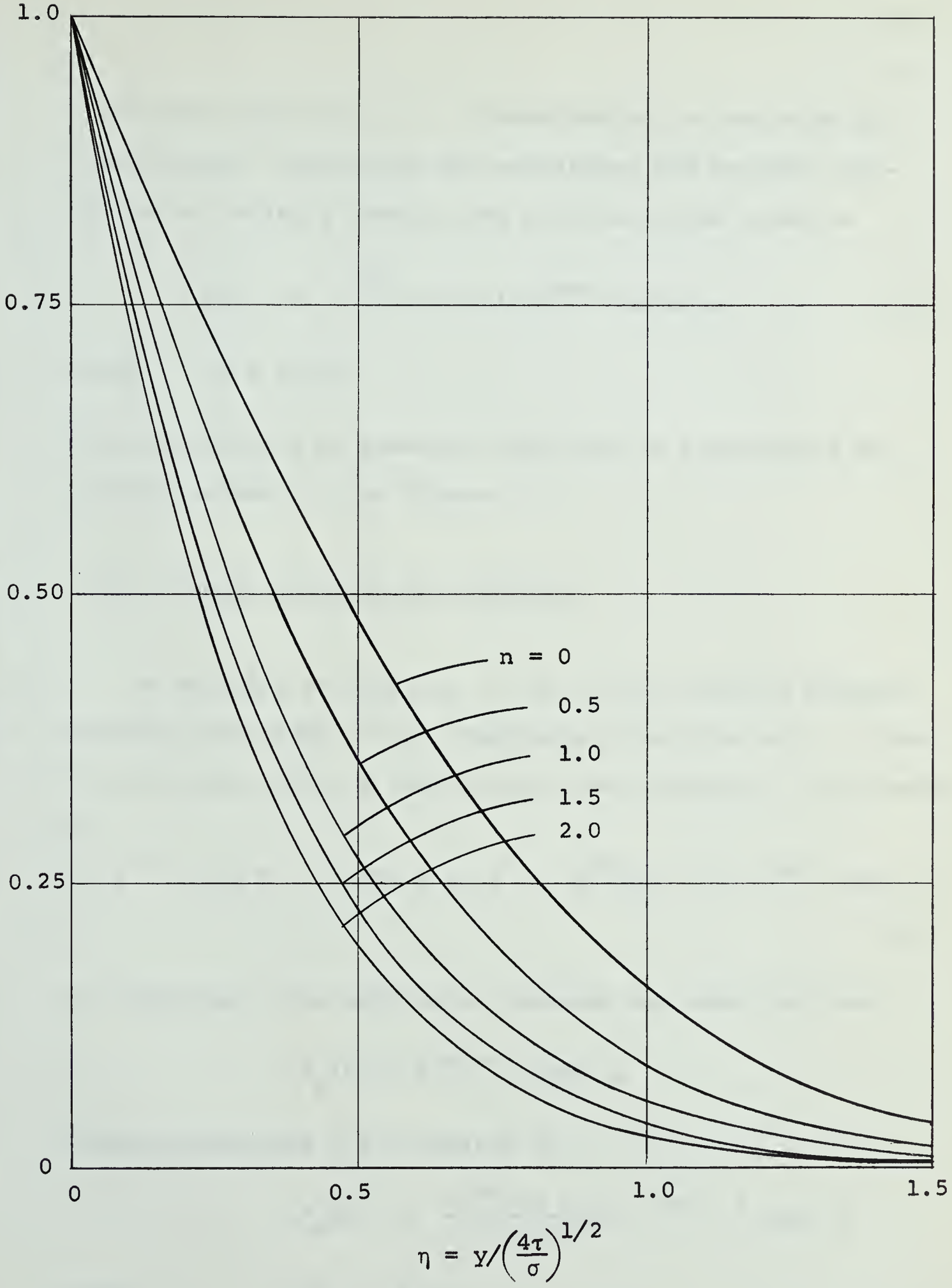

FIG. 2.2 TEMPERATURE PROFILES

consistent with $Q(\infty) = 0$. Substituting the solution for temperature, integrating and satisfying the boundary condition at infinity permits the solution to be given as

$$\Phi(\eta) = -2^{2n}\,\Gamma(n+1)\,i^{2n+1}\,\text{erfc}\,\eta, \qquad 2.2\text{-}6$$

where $2n = 0,1,2, \ldots .$

The distribution of pressure departure is illustrated for several values of n on figure 2.3.

2.2-3 Series Solution For Velocity

A solution of equation 2.1-20 is not possible without previous knowledge of the temperature distribution Φ. Since Φ is now available, a substitution into equation 2.1-20 leads to

$$\sigma F''' + 2\eta F'' - 2(2n+3) F' = -2^{2n}\Gamma(n+1)\, i^{2n+1}\,\text{erfc}\,\eta. \qquad 2.2\text{-}7$$

By inspection, the particular integral may take the form

$$F_p(\eta) \propto i^{2n+4}\,\text{erfc}\,\eta.$$

Substituting into 2.2-7 results in

$$F_p(\eta) = \frac{-2^{2n}\Gamma(n+1)}{(1-\sigma)}\, i^{2n+4}\,\text{erfc}\,\eta$$

where $2n = 0,1,2, \ldots .$

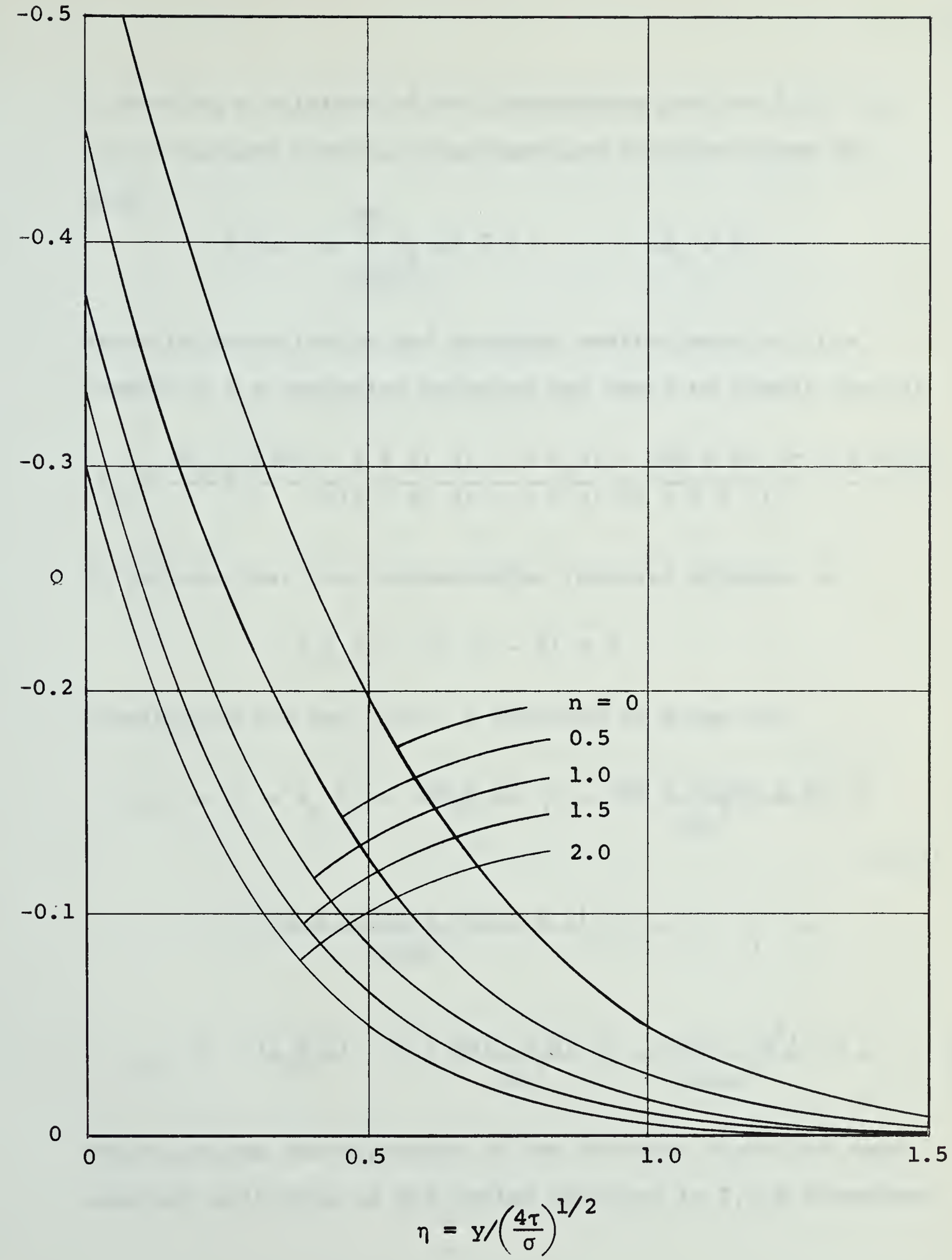

FIG. 2.3 PRESSURE PROFILES

In seeking a solution of the homogeneous part of 2.2-7, it may be assumed that the complementary function takes the form

$$F_c(\eta) = \sum_{m=0}^{\infty} d_m \eta^{m+\gamma} . \qquad (d_o \neq 0)$$

Hence by substituting and grouping coefficients of like powers of η a recursion relation may again be found; that is

$$d_r = \frac{-d_{r-2}\left[2(r-2+\gamma)(r-3+\gamma) - (4n+6)(r-2+\gamma)\right]}{\sigma(r+\gamma)(r-1+\gamma)(r-2+\gamma)} .$$

It follows that the corresponding indicial equation is

$$d_o\gamma(\gamma-1)(\gamma-2) = 0 .$$

Considering the zero root, a solution is given by

$$F_c(\eta) = d_o + d_1\left[\eta + \frac{(2n+3)}{3\sigma}\eta^3 + \frac{(2n+3)(2n+1)}{30\sigma^2}\eta^5 + \frac{(2n+3)(2n+1)(2n-1)}{630\sigma^3}\eta^7 + \ldots.\right] + \qquad 2.2\text{-}8$$

$$d_2\left[\eta^2 + \frac{(1+n)}{3\sigma}\eta^4 + \frac{4n(1+n)}{90\sigma^2}\eta^6 - \frac{2n(1-n^2)}{630\sigma^3}\eta^8 + \ldots.\right].$$

The solutions corresponding to the non-zero roots are again constant multiples of the series obtained in 2.2-8, therefore

2.2-8 is taken as the complete complementary solution. The total solution of 2.2-7 is then the sum of $F_p(\eta)$ and $F_c(\eta)$, namely

$$F(\eta) = d_o + d_1 \left[\eta + \frac{2n + 3}{3\sigma} \eta^3 + \frac{(2n + 3)(2n + 1)}{30\sigma^2} \eta^5 + \right.$$

$$\left. \frac{(2n + 3)(2n + 1)(2n - 1)}{630\sigma^3} \eta^7 + \ldots . \right] \qquad 2.2\text{-}9$$

$$+ d_2 \left[\eta^2 + \frac{(1 + n)}{3\sigma} \eta^4 + \frac{4n(1 + n)}{90\sigma^2} \eta^6 - \frac{2n(1 - n^2)}{630\sigma^3} \eta^8 + \ldots . \right]$$

$$- \frac{2^{2n} \Gamma(n + 1)}{(1 - \sigma)} i^{2n + 4} \operatorname{erfc} \eta .$$

Satisfying the first boundary condition $F(0) = 0$ requires that

$$d_o = \frac{\Gamma(n + 1)}{16\Gamma(n + 3)(1 - \sigma)} ,$$

and similarly satisfying $F'(0) = 0$ requires

$$d_1 = \frac{\Gamma(n + 1)}{16\Gamma(n + \frac{5}{2})(1 - \sigma)} .$$

The remaining boundary condition, $F'(\infty) = 0$, is found to give

$$d_2 = \frac{-2^{2n}\Gamma(n + 1)}{8\Gamma(n + 2)(1 - \sigma)}$$

by successive application of Euler's transformation on the first two infinite series of 2.2-9. A single differentiation of 2.2-9 then gives the velocity distribution in closed form as

$$F'(\eta) = \frac{\Gamma(n+1)}{\Gamma(n+\frac{5}{2})\,(1-\sigma)}\left[1 + (2n+3)\left(\frac{\eta}{\sqrt{\sigma}}\right)^2 + \frac{(2n+3)(2n+1)}{6}\left(\frac{\eta}{\sqrt{\sigma}}\right)^4 + \ldots\right] - \frac{2^{2n}\,\Gamma(n+1)}{8\Gamma\,(n+2)(1-\sigma)}$$

$$\left[2\left(\frac{\eta}{\sqrt{\sigma}}\right) + \frac{4(1+n)}{3}\left(\frac{\eta}{\sqrt{\sigma}}\right)^3 + \frac{4n(1+n)}{15}\left(\frac{\eta}{\sqrt{\sigma}}\right)^5 + \ldots\right]$$

$$+ \frac{2^{2n}\,\Gamma(n+1)}{(1-\sigma)}\; i^{2n+3}\mathrm{erfc}\;\eta\;,$$

from which it follows that

$$F'(\eta) = \frac{2^{2n}\,\Gamma(n+1)}{(1-\sigma)}\left[i^{2n+3}\mathrm{erfc}\;\eta - i^{2n+3}\mathrm{erfc}\left(\frac{\eta}{\sqrt{\sigma}}\right)\right]. \qquad 2.2\text{-}10$$

The velocity distribution is illustrated for selected values of n on figure 2.4 for water and on figure 2.5 for glycerine. On both diagrams, the temperature profile (n = 1) is given for reference.

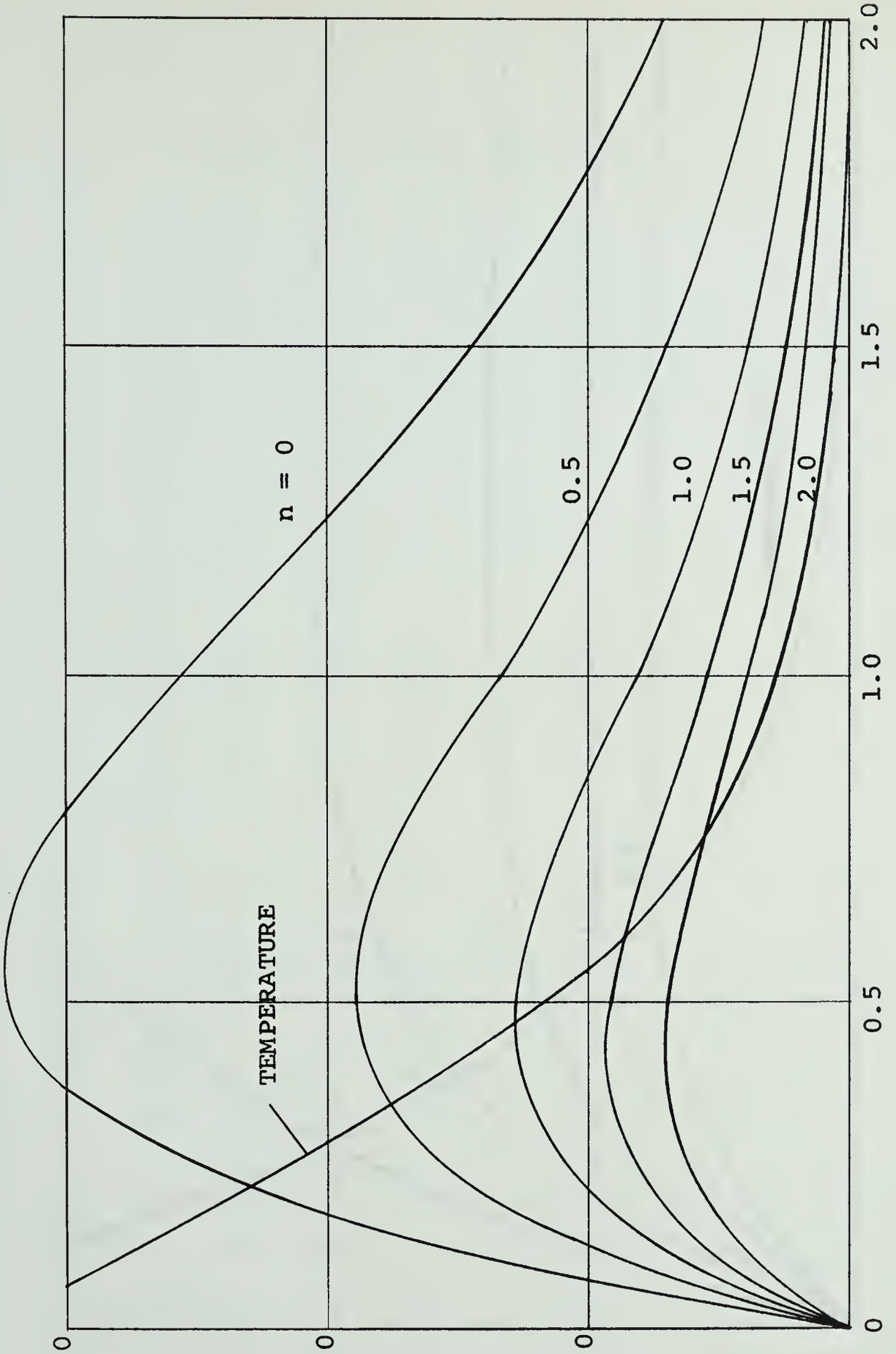

FIG. 2.4 VELOCITY PROFILES ($\sigma = 5.9$)

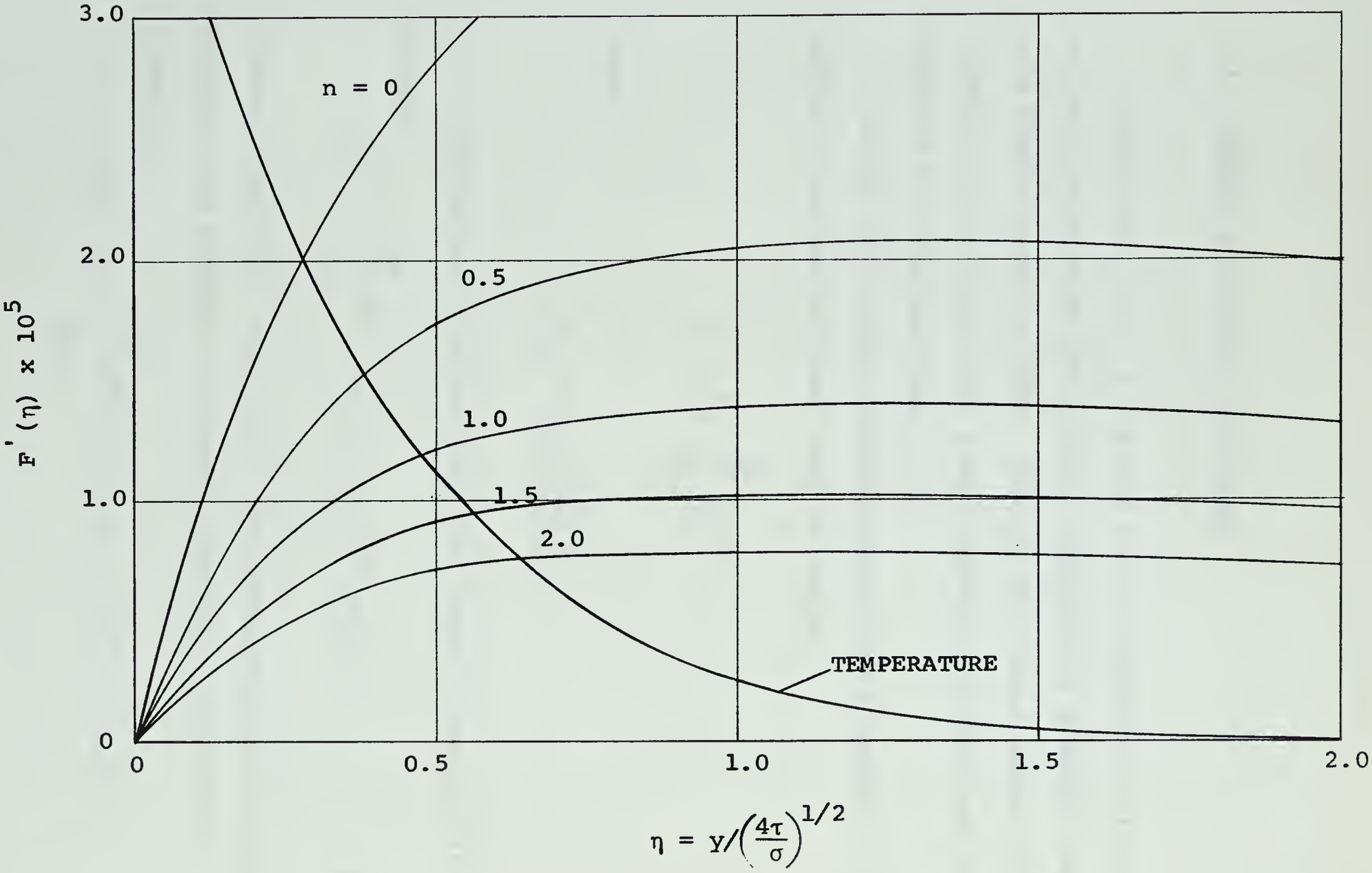

FIG. 2.5 VELOCITY PROFILES (σ = 2500)

2.3 GENERAL LINEARIZED SOLUTIONS

Equations 2.2-3, 2.2-6 and 2.2-10 represent solutions to the problem when the surface temperature gradient varies as a simple power of time. Due to the linear nature of the boundary layer equations, a more general solution may be obtained by superposition.

Assume the surface temperature can be expanded in a Maclaurin series of time; that is taking

$$\zeta = x \sum_{s=0}^{\infty} b_s \tau^s$$

where

$$b_s = \frac{1}{s!} \left(\frac{d^s z}{d\tau^s} \right)_{\tau=0} .$$

It is immediately apparent that the temperature distribution becomes

$$\Phi(\eta) = \sum_{n=0}^{\infty} 2^{2n} \Gamma(n+1) b_n i^{2n} \operatorname{erfc} \eta . \qquad 2.3\text{-}1$$

Substituting 2.3-1 into 2.2-5, the pressure distribution for the same arbitrary surface temperature gradient is given by

$$Q(\eta) = -\sum_{n=0}^{\infty} 2^{2n} \Gamma(n+1) b_n i^{2n+1} \operatorname{erfc} \eta .$$

A similar substitution of Φ into 2.1-20 may be used to show that the velocity profile is

$$F'(\eta) = \frac{1}{(1 - \sigma)} \sum_{n=0}^{\infty} 2^{2n}\, \Gamma(n + 1)\, b_n \left[i^{2n+3}\mathrm{erfc}\ \eta - i^{2n+3}\mathrm{erfc}\left(\frac{\eta}{\sqrt{\sigma}}\right)\right] .$$

CHAPTER III

EXPERIMENTAL WORK

3.1 DESIGN OF APPARATUS

In view of the approximations made for the linearized theory in Chapter II, experiments were necessary to establish their validity over the range of conditions considered for similarity.

A pictorial view of the apparatus used is given in figure 3.1 and a detail view in figure 3.2. It consisted of a 25 x 6 x 12 inch tank of transparent walls (Perspex), the base of which was in the form of a flat opaque plastic (Teflon). This plate, it was felt, would permit the establishment of temperature gradients longitudinally at the surface with negligible conduction losses for the duration of a test.

Differential heating of the surface was achieved by means of thermoelectric cooling modules which were controlled by a series of Ohmite adjustable resistors. A typical module is shown in figure 3.3. It is rated at 22.2 watts for a maximum current of thirty amperes when the hot side is maintained at 27 °C and the cool side is thermally insulated. An electrically insulating film on both sides eliminated the possibility of a short circuit. In all, thirty six modules

FIG. 3.1 GENERAL VIEW OF APPARATUS

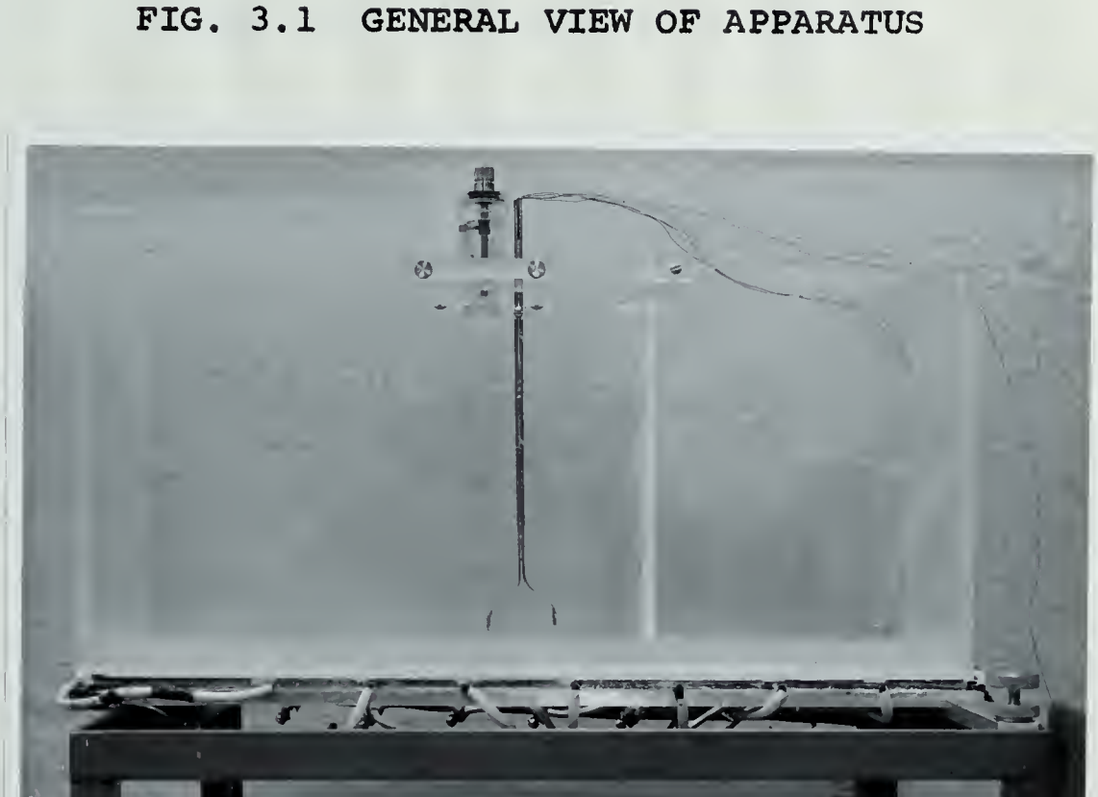

FIG. 3.2 DETAIL VIEW OF TANK

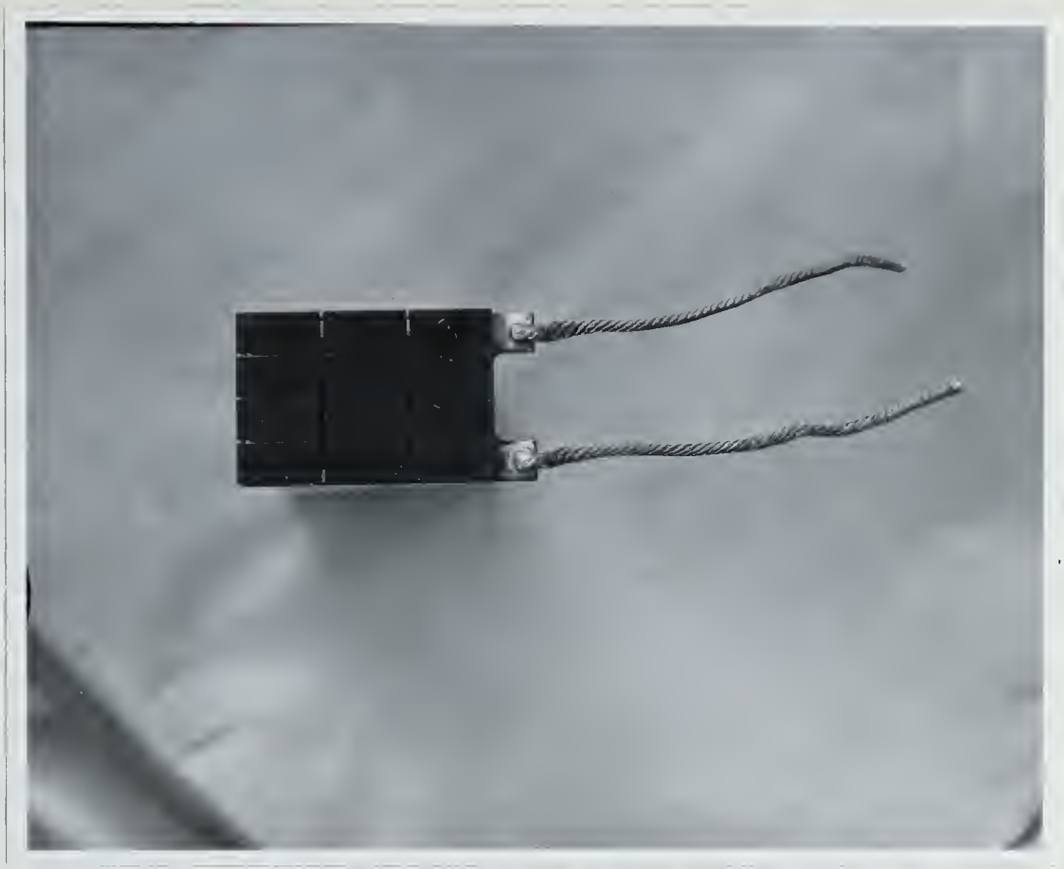

FIG. 3.3 PLAN VIEW OF A MODULE

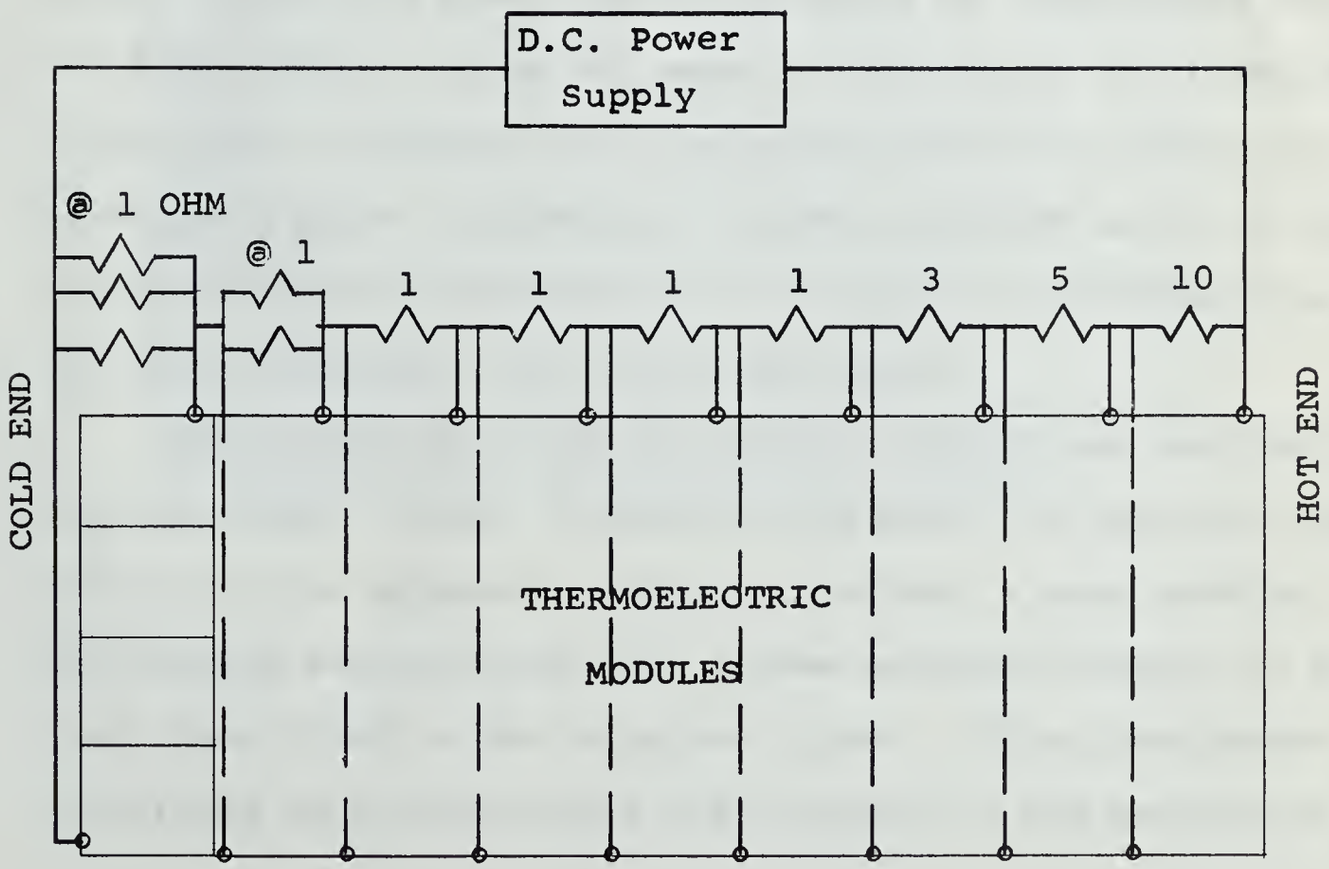

FIG. 3.4 SCHEMATIC OF HEATING CIRCUIT

were needed. These were arranged in sets of four laterally and connected to the resistors as shown on the schematic diagram 3.4. A Hewlett Packard D.C. power supply rated at forty five amperes and eighteen volts was utilized to provide the necessary power. Due to the apparent linear behavior of the modules and a fine degree of adjustment on the resistors, a wide range of linear rates of heating could be obtained at the surface of the teflon plate.

To support the modules and the tank, a 26 x 6 7/8 x 18/32 inch aluminum plate was selected on the basis of its high thermal capacity and its low specific weight. Considering the plate as a simply supported beam carrying a uniform distributed load, a maximum centerline deflection of 0.003 inches had been calculated based on anticipated depths of fluid (three inches of water or two inches of glycerine). Additional stiffness was introduced by the four walls of the tank and further stiffening ribs were mounted on the outside of the tank and therefore it was felt that the deflection of the horizontal surface was negligible.

The levelling of the horizontal surface was carried out in two steps. First, a course adjustment was obtained with screws on the apparatus stand and second, a more precise adjustment was achieved with screws mounted directly on the tank base (that is the aluminum plate). This arrangement permitted an accuracy of $\pm$ 0.25 minutes in the setting of

the level longitudinally with the levelling device of figure 3.5. Because of its length, this device could not be placed fully in a lateral position, hence an accurate setting of the lateral level of the teflon surface could not be achieved. In view of the isothermal condition laterally and temperature gradients existing only longitudinally, it would seem that this is not critical (see Appendix C).

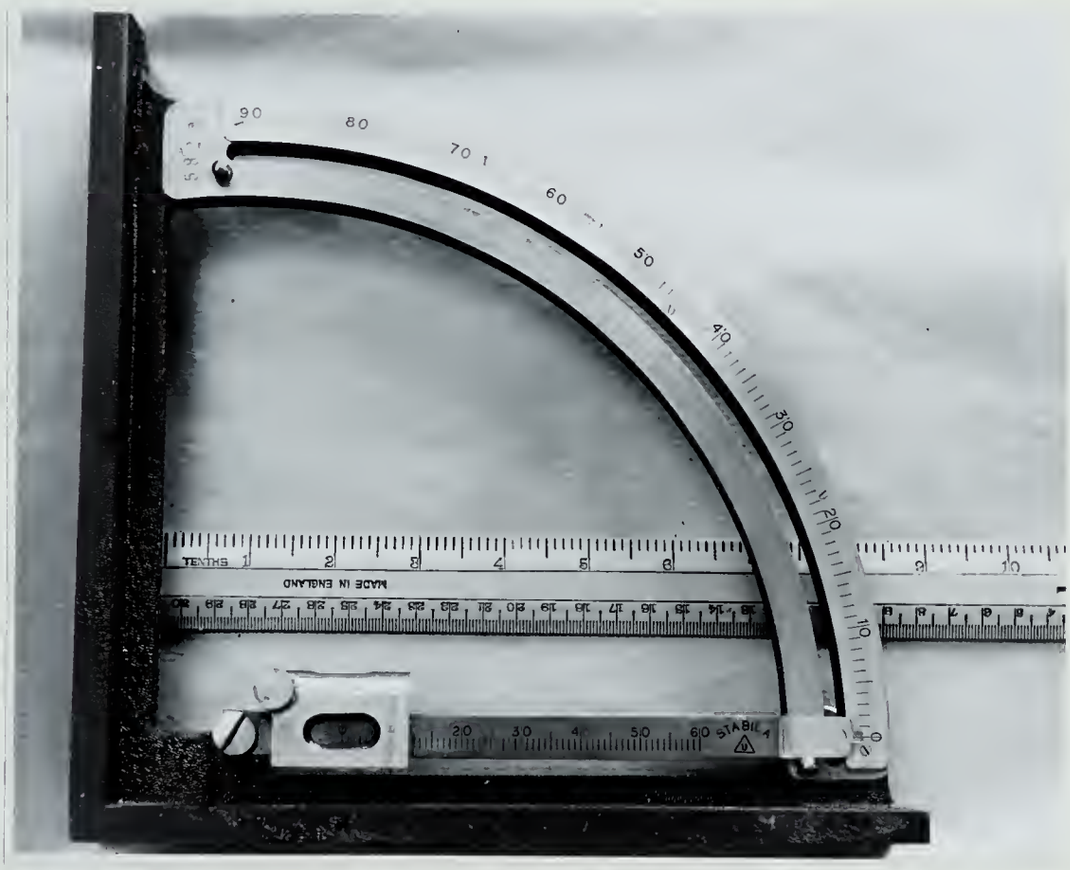

FIG. 3.5 LEVELLING DEVICE

3.1-1 Assembly of Plate

One of the critical points in the design of the apparatus was the flatness of the horizontal surface. Initially the supporting aluminum plate was machined on both sides to a flatness of ± 0.001 inches. Then the thermoelectric cooling modules were bonded to the plate with an Epoxy resin cement. Following this, a coat of teflon bonding cement was applied on the opposite side of the modules, then a 0.070 inch thick teflon sheet was clamped to the modules. As a final step, this "sandwich" was machined only on the teflon side until the upper surface and lower surface were parallel to within ± 0.001 inches. Local roughness on the teflon surface was minimized by polishing with emery paper to a smooth finish.

3.2 INSTRUMENTATION

From the similarity analysis of Chapter II, it was predicted that solutions to the governing equations are possible provided a linear temperature distribution is imposed at the surface. Experimentally, this gradient could be obtained by simultaneous manipulation of the adjustable resistors in parallel with the modules. To determine the actual temperature of the surface, nine evenly spaced thermocouples were imbedded in the teflon. 0.020 x 0.025 inch grooves were cut

laterally into the surface using a scriber such that the thermocouples could be placed along isothermals (noting that the apparatus had been constructed to give nearly isothermal conditions traversely). Honeywell Type-J iron-constantan (0.010 inches in diameter) thermocouples joined by a lap weld were used.

All of the above mentioned thermocouples were connected to a switching unit whose single output was then recorded on a Varian single channel strip chart recorder. An actual speed of sixteen inches of paper per minute with a full scale deflection of one millivolt in 0.5 seconds permitted temperature transients to be recorded with a response of 60 $^{\circ}$F/sec.; uncertainty in reading the strip chart recordings was $\pm$ 0.10 $^{\circ}$F.

Temperatures in the water near the Teflon surface (that is in the boundary layer) were also measured by thermocouples. These were identical to those mentioned previously except a butt weld was used to join the two dissimilar metals. In all, four thermocouples were mounted in a staggered manner on a common stem, the position of which could be accurately controlled with a micrometer screw mounted on top of the tank. A resolution of $\pm$ 0.0005 inches in locating thermocouples from the surface permitted a sufficient number of temperature recordings to be taken over a relatively small distance (that is over anticipated boundary layer thicknesses of 0.10 inches). These thermocouple

responses were recorded on two single channel strip chart recorders, identical to that mentioned above. Bulk fluid temperatures were determined by four mercury-in-glass thermometers which were located at the inside corners of the tank such that they would not disturb the main flow.

3.3 EXPERIMENTAL METHOD

As evident from the theoretical predictions of Chapter II, the linearized theory is applicable to fluids in a large range of Prandtl numbers. Since it is neither desirable nor possible to investigate all fluids, experiments were performed only in water, glycerine and air.

The theoretical predictions also embrace a wide range of temporal variations of the surface temperature. One which is relatively easy to set up in a laboratory is the linear variation, hence it was decided to carry out experiments imposing linear surface temperatures with respect to both time and position along the plate. This then fixes the temperature index n at unity resulting in c being the only parameter for all tests.

3.3-1 Testing Program

In order to obtain a sufficient amount of experimental data, the experimental schedule was carried out in two

phases. First, a number of investigations were made in different fluids to determine the validity of the approximations for the linearized theory. Then tests were undertaken to determine the uncertainty in the main test results.

Main Schedule:

(a) Initially, experiments were made in water for three different values of c which not only provided results but also gave an indication of the limits of the apparatus and the time taken for leading edge effects to propagate along the plate.

(b) Secondly, a test in glycerine was performed to gain knowledge about the behavior of the flow for at least one large Prandtl number.

(c) Finally, an investigation in air was made to determine whether or not a radiation heat loss was appreciable.

Supplementary Tests Schedule:

(a) Since a change in angle (with respect to the horizontal) of the working surface may have an effect on the main flow, a test in water at c = 0.34 °F/ft. sec. was made for various angles.

(b) A final auxiliary test was carried out in water for various depths of fluid to determine the effect of back flow.

3.3-2 Preliminary Tests

Difficulties (due to the delicacy of the thermoelectric modules) during the initial trial runs led to malfunctions in a few modules. Consequently, the working section had to be reduced from an initial length of twenty five inches to a final length of fifteen inches by inserting a baffle at one end of the tank. This was found adequate for test purposes.

At an advanced stage in the experiments with water, the surface thermocouples gave erratic readings. Initially, those at the hot end of the plate became unreliable and eventually all of the surface thermocouple readings became irregular. This, it is believed, can be attributed to differential expansion between the thermocouples, cement and teflon ultimately leading to the separation of the junctions. The probe thermocouples were therefore used in both setting boundary conditions and in the measurement of temperatures in the boundary layer.

3.3-3 Test Procedure

Considering a test in water the procedure (which was the same for all runs) consisted of the following steps. Utilizing one of the probe thermocouples, the surface temperature was adjusted (by varying the power supply to sets

of modules) such that it varied both linearly with respect to position along the plate and time. Typical surface temperature distributions at various times are illustrated on figure 3.6 for c = 0.49 °F/ft. sec. The apparatus was then allowed to stand undisturbed at room temperature until it was considered to be isothermal throughout. The probe thermocouple was then located in the boundary layer region and a strip chart recorder was started. Switching on the power supply immediately after this, a "blip" appeared on the strip chart providing an excellent timing mark. The temperature was then continuously recorded until a definite change in the linear behavior was observed (indicating the onset of a leading edge effect).

Since each temperature was measured at only one point at a time all of the curves were superimposed until the "blips" coincided hence giving reference to the same temporal origin. The reproducibility of the curves was found to be good.

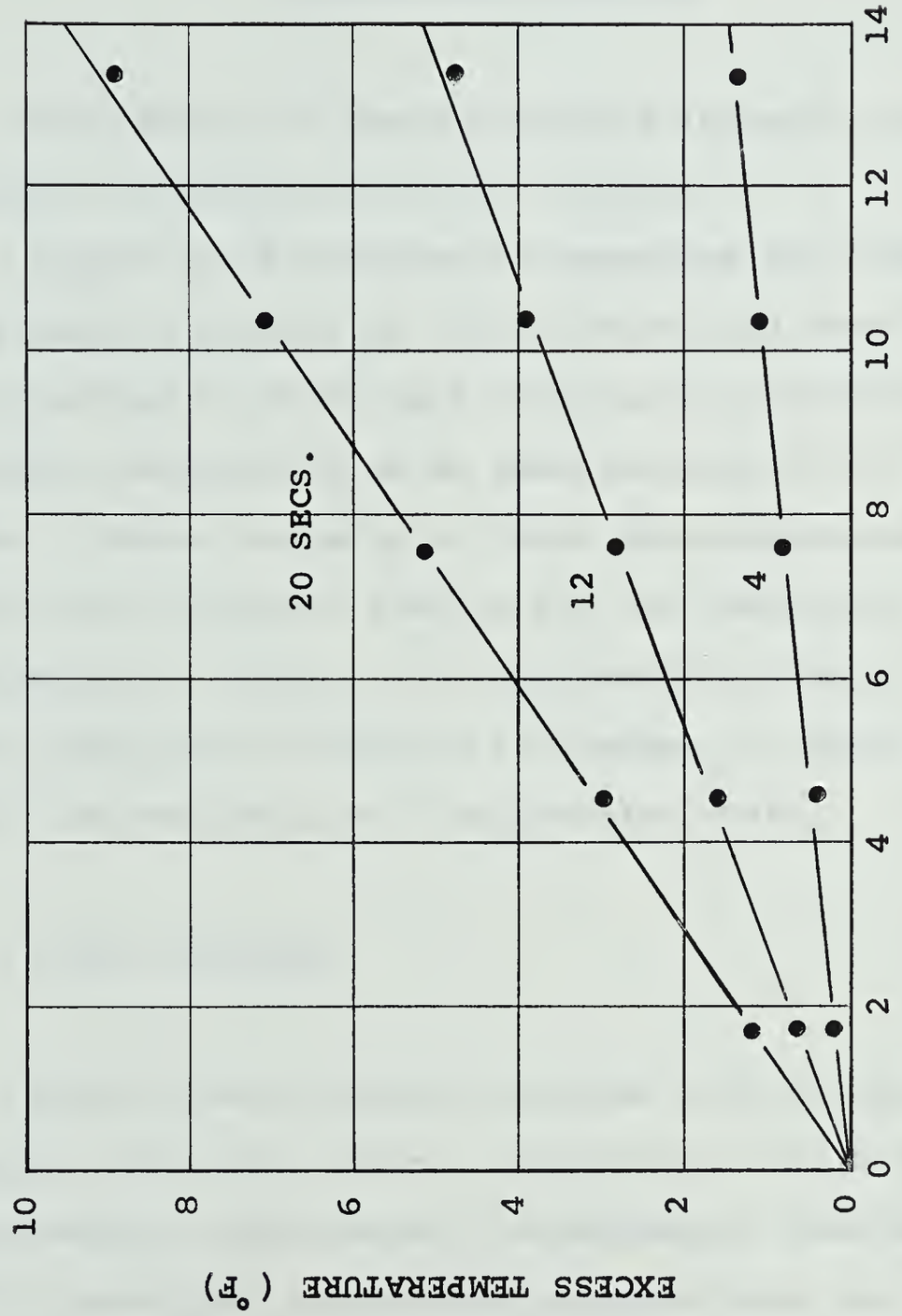

FIG. 3.6 TYPICAL SURFACE TEMPERATURE PROFILE

CHAPTER IV

EXPERIMENTAL RESULTS

The results of tests performed in water, glycerine and air are presented in this chapter.

A spot check obtained by immersing the thermocouple in firstly a mixture of ice and water and then boiling water, the readings of which were taken on a potentiometer, read the same temperature as an immersed mercury-in-glass thermometer. Hence, assuming a linear correspondence between the strip chart recorder reading and the temperature at the thermocouple junction, all intermediate changes in millivolt output were converted to changes in temperature by using the manufacturer's calibration chart.

4.1 TESTS IN WATER

Having used ordinary tap water with no special preparation other than natural de-aeration over a twenty four hour period, comparisons of experimental results obtained with theoretical temperature distributions are given in figures 4.1, 4.2 and 4.3. A sample calculation of the conversion of the strip chart recordings may be found in Appendix D. Figure 4.1 illustrates typical variations of temperature with time at various positions from the surface (for $c = 0.34\,^{\circ}F/ft.\ sec$).

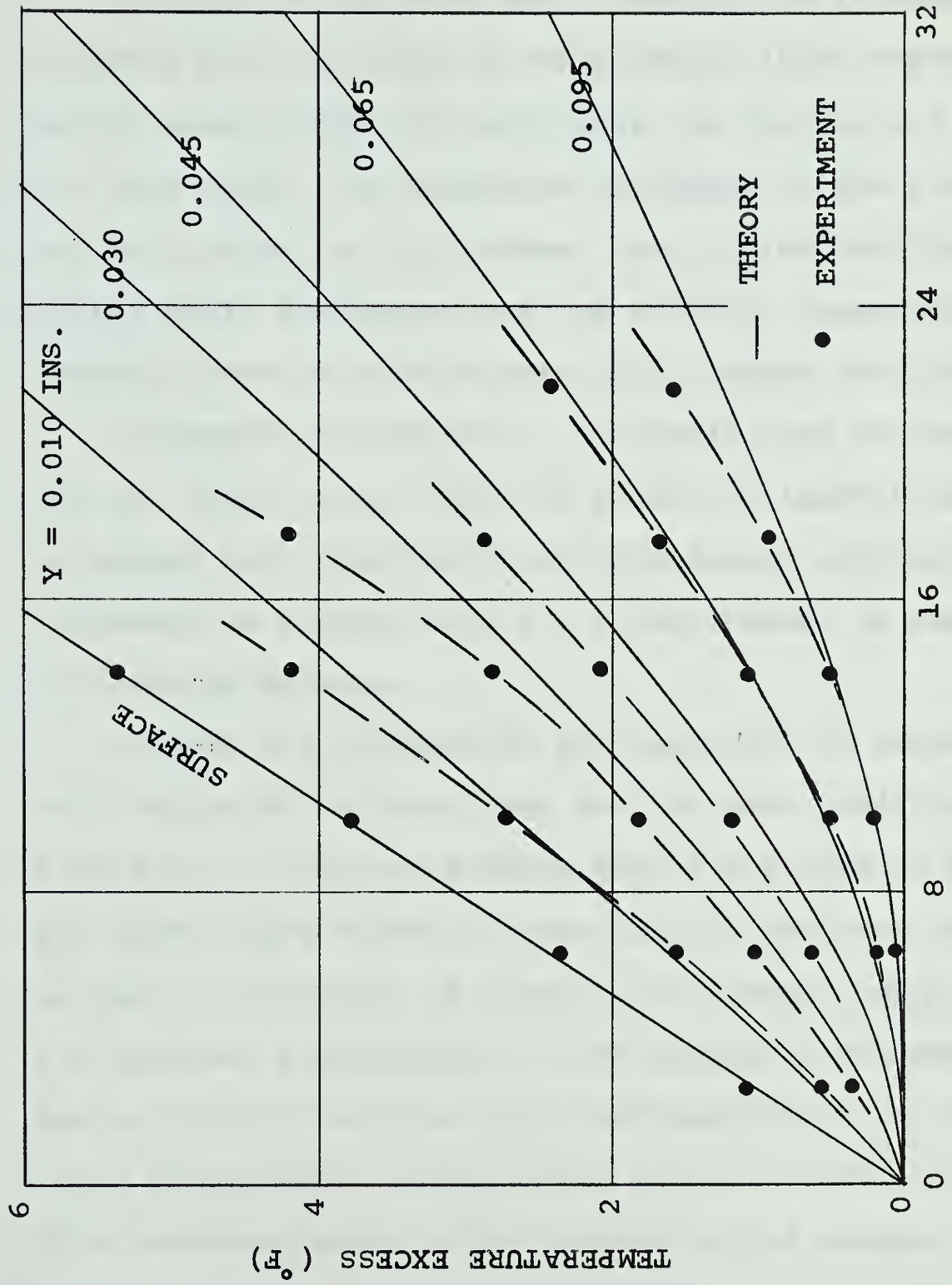

FIG. 4.1 VARIATION OF TEMPERATURE WITH TIME

In view of the very small temperature increases associated with the edge of the boundary layer where experimental errors might be very large, no results are given for this range. An estimated thickness of the thermal boundary layer is 0.12 inches. Due to inaccuracies in estimating small distances from the surface, temperature measurements were not made within 0.010 inches from the surface.

Agreement in figure 4.1 is mostly good for small times but for large times, when the effect of inertia is expected to become more important, the discrepancy increases. The agreement is poorest near y = 0.040 inches, in the region of velocity maximum.

Figure 4.2 illustrates the variation of temperature with height at various times for the same conditions as in figure 4.1. Near the surface and at the edge of the boundary layer where viscous forces tend to dominate agreement is good. The effect of inertia, if present, would assume its greatest significance in the region of maximum velocity. Due to inertia the flow might be expected to be retarded hence experimental temperatures would lie above theory. This certainly seems to be evident in the maximum velocity region of figure 4.2 where the discrepancy, although not large, is greatest. Temperature recordings are not shown for larger times than sixteen seconds due to an onset of a leading edge effect as discussed in Chapter 5, section 5.2.

The non-dimensional temperature profiles for two tests

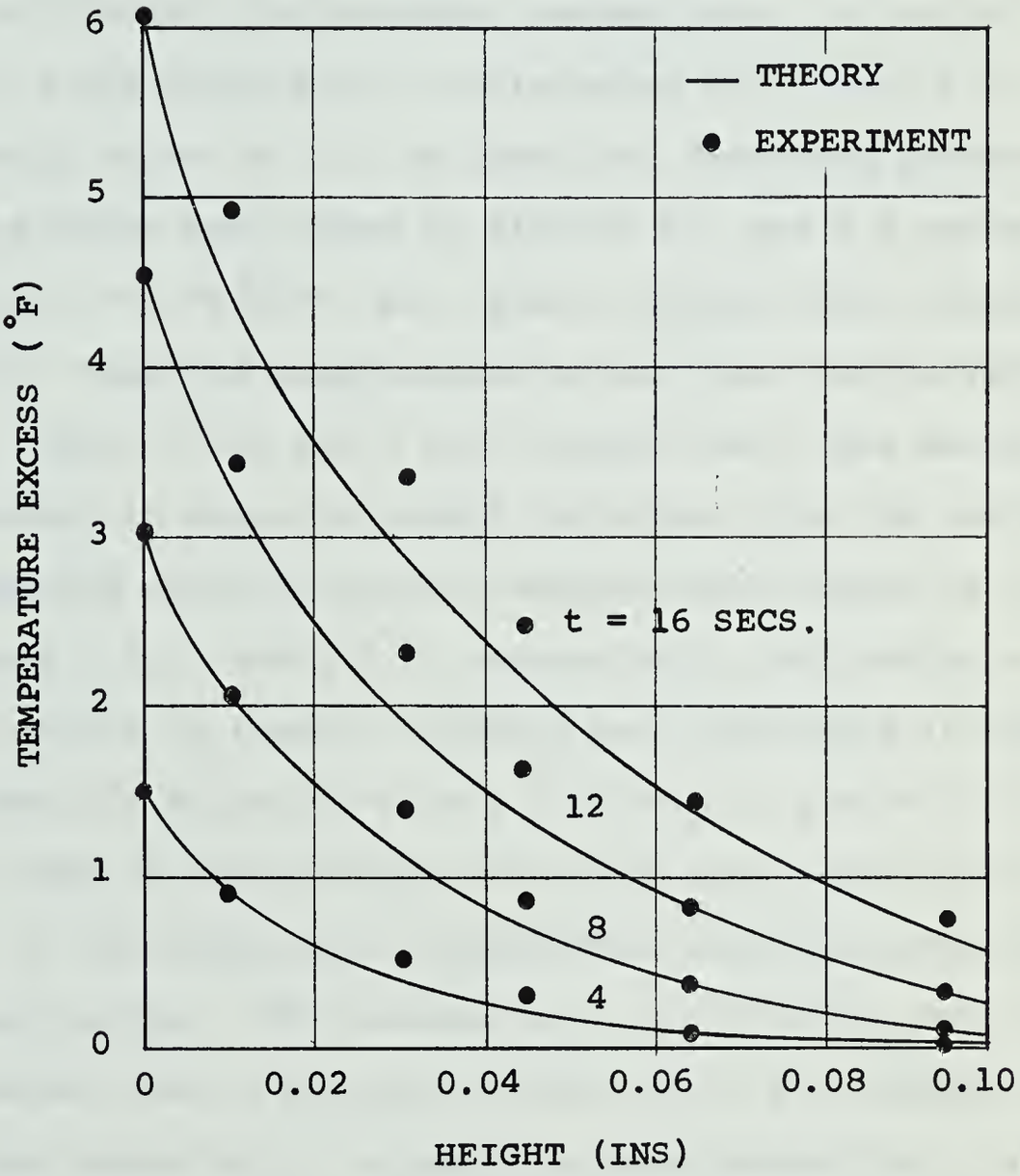

FIG. 4.2 VARIATION OF TEMPERATURE WITH HEIGHT

are compared with the linearized theory (n = 1) in figure 4.3. A third test (c = 0.49 °F/ft. sec.) gave erratic date due, it is thought, to incipient instability: it is not included in the results but is discussed in section 5.4. The velocity curve (n = 1) is given for reference purposes. The points which were shown in figures 4.1 and 4.2 corresponding to c = 0.34 °F/ft. sec. again indicate fair overall agreement. Possible experimental errors near the surface in Φ and η are $\pm$ 0.04 and $\pm$ 0.02 respectively, due mainly to inaccuracy in measuring small distances from the surface. In the maximum velocity region, experimental errors in Φ and η are about $\pm$ 0.04 and $\pm$ 0.02 respectively, indicating a possible effect of inertia although not confirming it definitely. Possible errors in Φ of $\pm$ 0.02 and in η of $\pm$ 0.02 near the edge of the boundary layer are mainly due to inaccuracy in detecting small temperature increases associated with these points. The results for c = 0.27 °F/ft. sec. show good agreement over the entire profile with the exception of the largest value of η. A possible experimental error in Φ of $\pm$ 0.02 in this region again is a result of inaccuracy in estimating small temperature increases.

A fourth test (c = 0.34 °F/ft. sec.) performed at a distance of seven inches from the leading edge was in similar agreement with the theory. Since no additional information about the effect of inertia could be obtained, it was not included in this thesis.

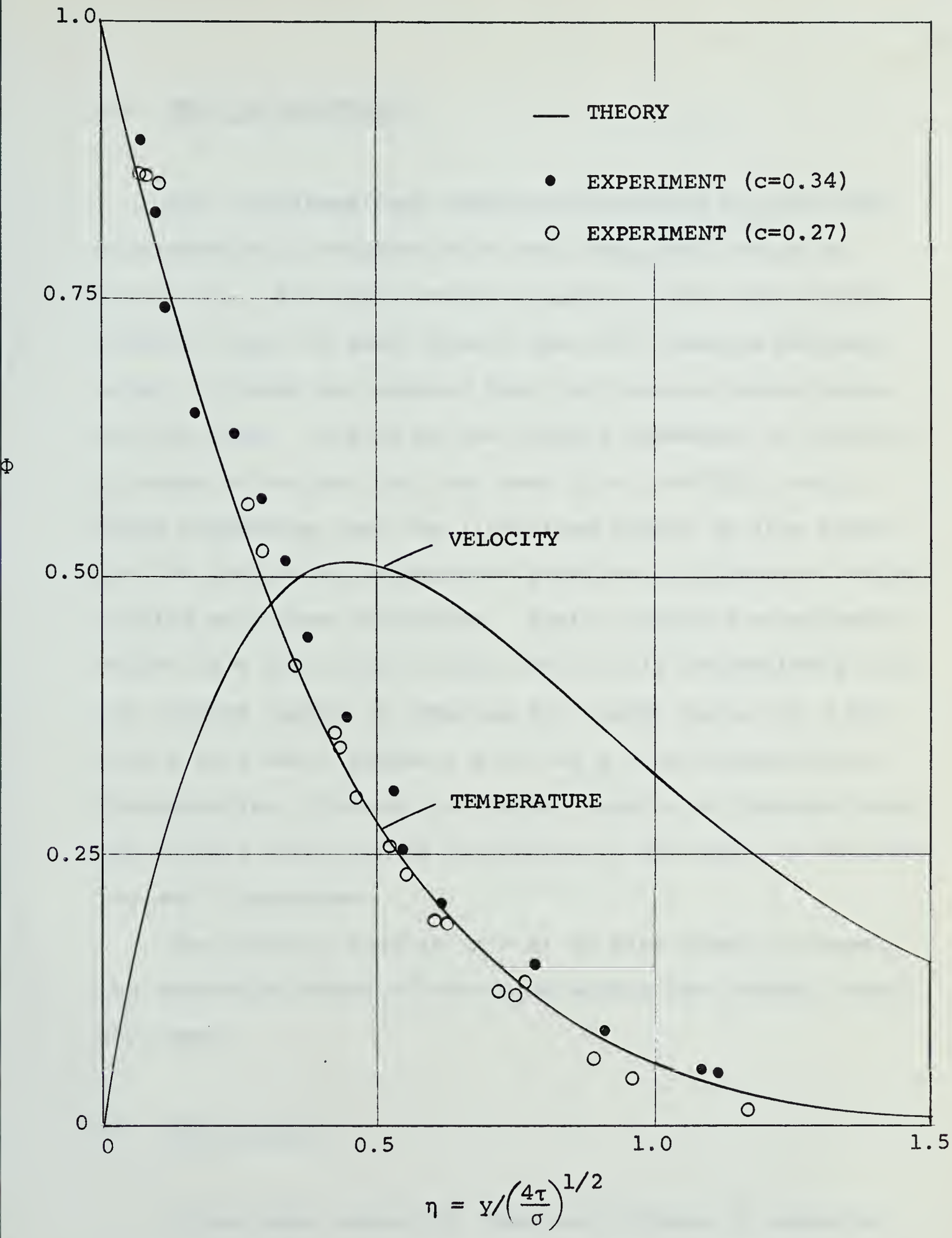

FIG. 4.3 COMPARISON OF TEMPERATURE PROFILES (WATER)

4.2 TEST IN GLYCERINE

The non-dimensional temperature profile for one test in glycerine is compared with the linearized theory in figure 4.4. For large Prandtl numbers, where the thermal boundary layer is much thinner than the momentum boundary layer, it might be expected that the viscous forces dominate the flow. In view of the overall agreement it certainly seems to be true for this test ($c = 0.49\,^{\circ}F/ft.\ sec.$), hence suggesting that the linearized theory is also adequate for predicting temperature profiles in glycerine during leading edge free conditions. Again, possible experimental errors in Φ and η are $\pm$ 0.030 and $\pm$ 0.015 respectively near the surface (small η), whereas for larger values of η the errors in Φ and η become $\pm$ 0.20 and $\pm$ 0.020 respectively. Discrepancies, although not large, seem to be greatest near the surface which can be attributed to the error in estimating small distances.

The velocity profile (n = 1) is also given to reveal the monotonic nature of the curve within the thermal boundary layer.

4.3 TEST IN AIR

It has been shown (16) that the effects of radiation losses in air for free convection on an inclined plate are

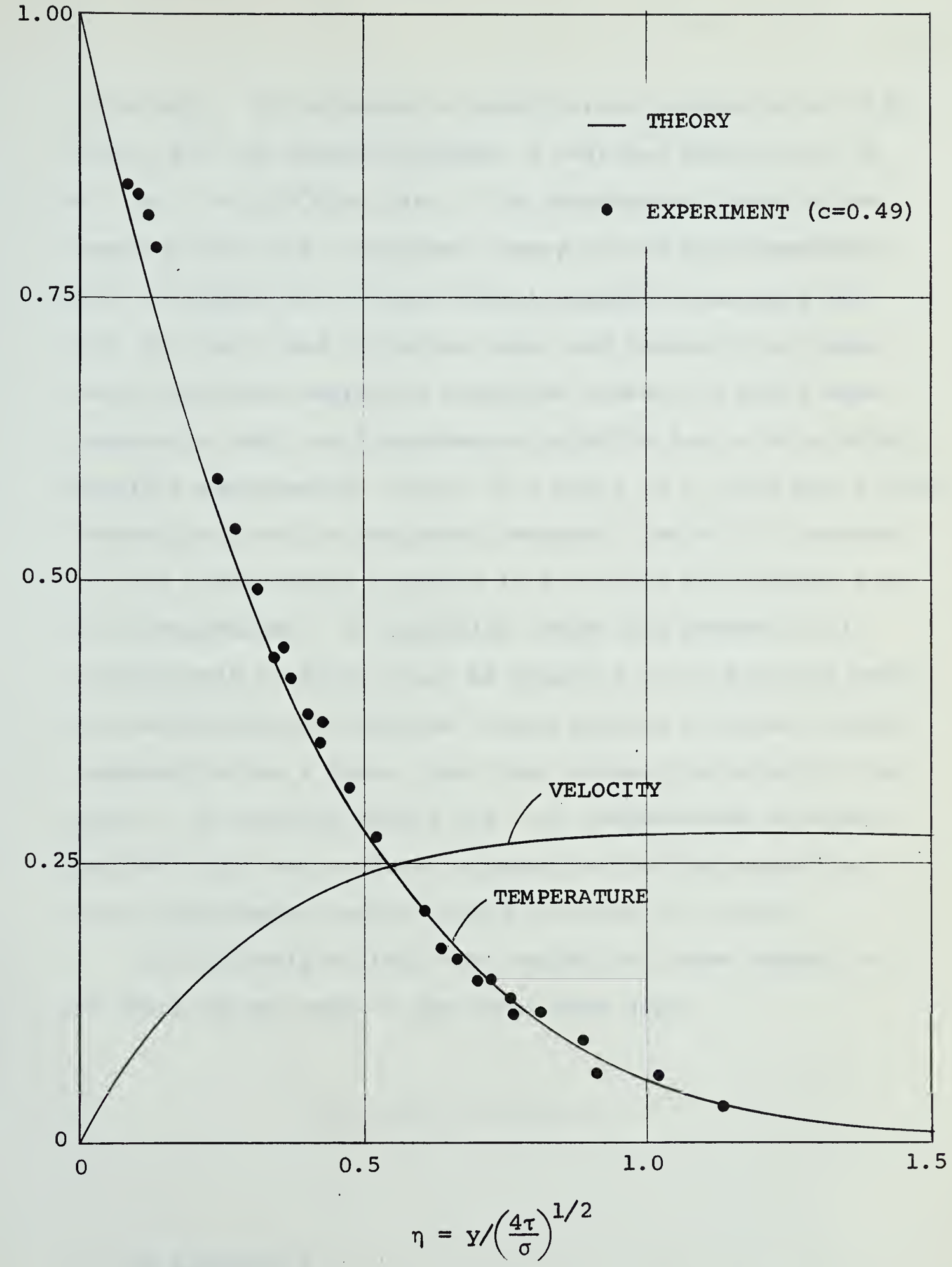

FIG. 4.4 COMPARISON OF TEMPERATURE PROFILES (GLYCERINE)

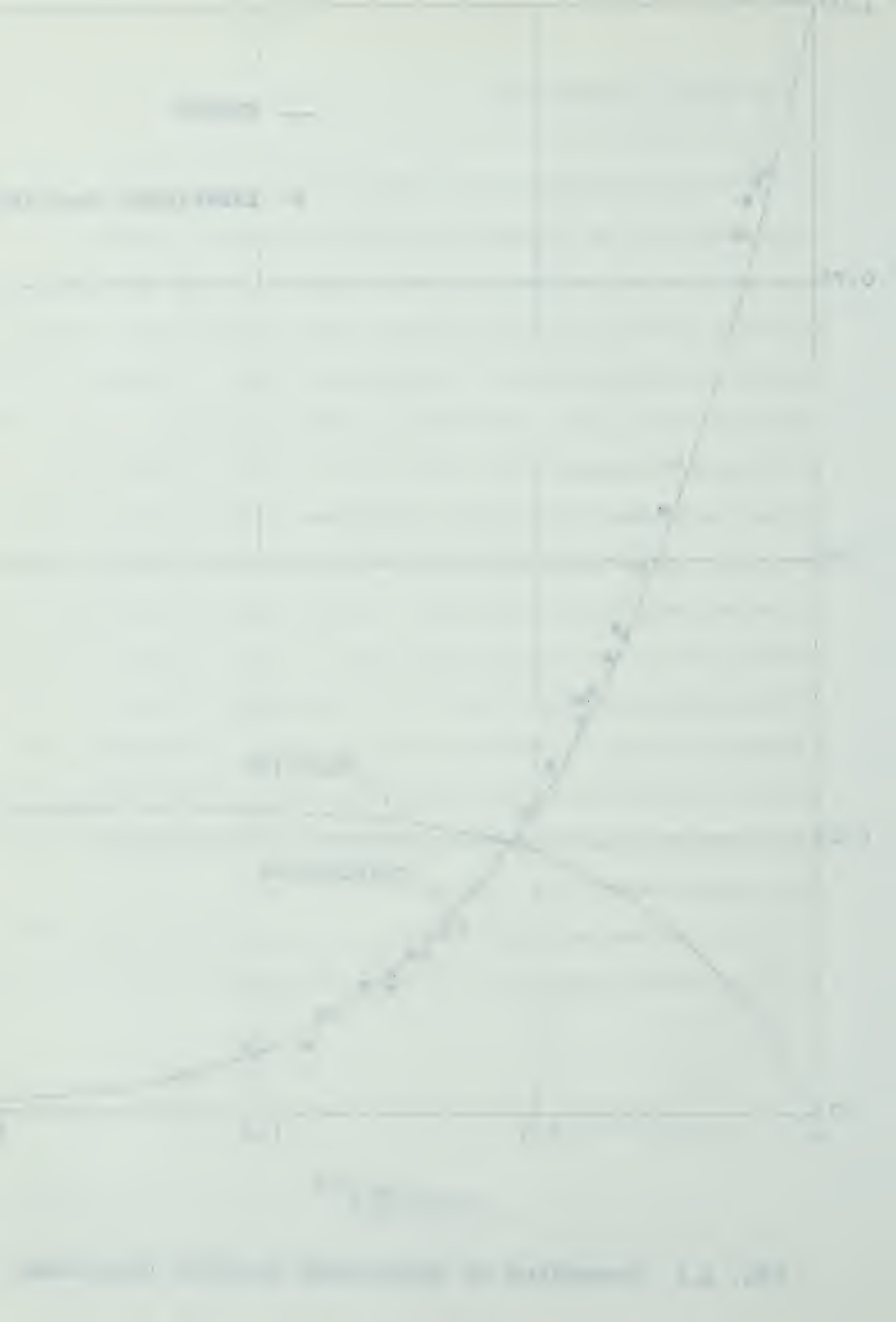

quite high. To determine a quantitative indication of this effect for the present problem, a test was carried out in air for c = 0.52 °F/ft. sec. The experimental results are compared with the linearized theory on the non-dimensional plot of figure 4.5. Since overal agreement was good for both the water and glycerine tests and because the linearized theory has neglected radiation losses, it would seem reasonable that the disagreement might be due to this effect. Possible experimental errors in Φ and η of $\pm$ 0.030 and $\pm$ 0.020 respectively and an estimated response time of 0.5 seconds for the thermocouple junction in air would not account for the disagreement. If radiation losses are present, all thermocouple readings would be expected to be high and hence the extrapolation technique* would predict a higher surface temperature (at a given time) than actually existed on the plate. In plotting figure 4.5, all temperatures were normalized with this surface temperature thereby suggesting that experimental results would be below the theory.

On the basis of this test radiation losses appear to be about 50 per cent of the total heat loss.

---

* see Appendix D.

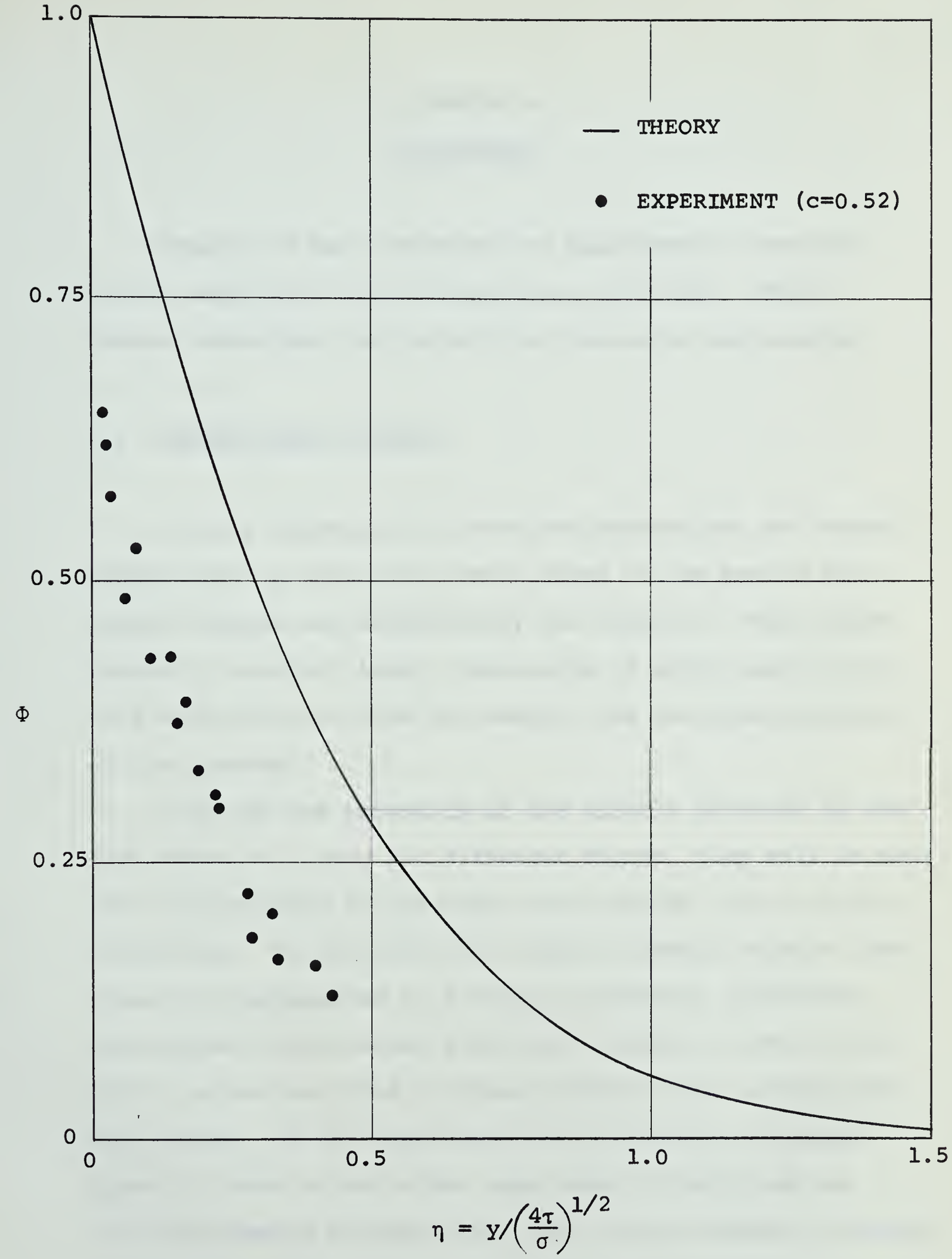

FIG. 4.5 COMPARISON OF TEMPERATURE PROFILES (AIR)

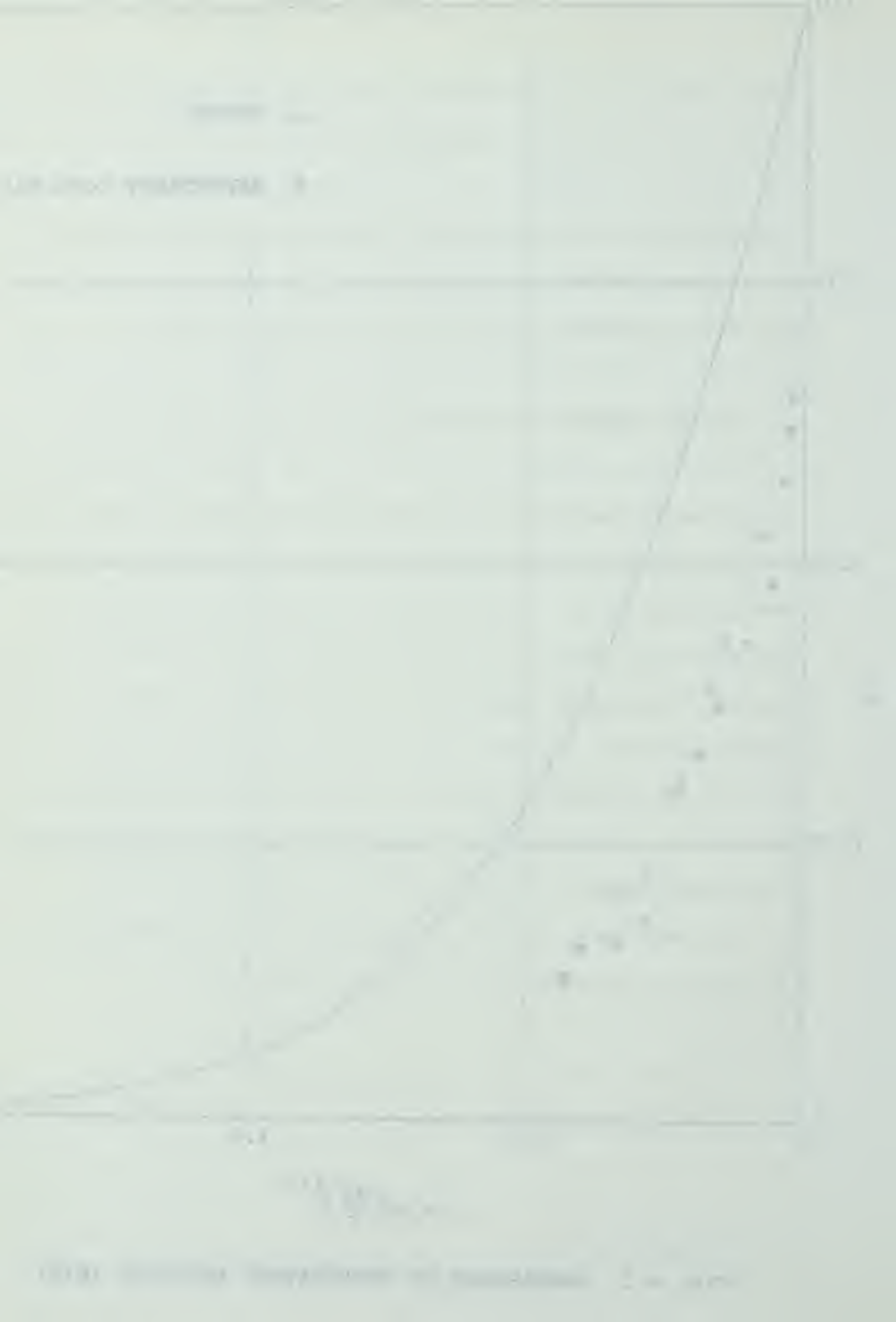

CHAPTER V

DISCUSSION

Chapter IV has presented the experimental results of the main tests with a discussion of errors. This chapter considers the validity in the main test results.

5.1 LATERAL EDGE EFFECTS

A tacit assumption in both the theoretical and experimental work is that the lateral edges of the heated horizontal surface are sufficiently far removed. These edges promote a boundary layer, the growth of which could interfere with the main flow and destroy the two-dimensionality of the problem.

Although the intensity of the effects produced by the side edges will vary for different fluids, they will in general be minimized if the edges are designed for the worst conditions. To eliminate any direct buoyancy effects, the edges were maintained at a nearly isothermal condition. Anticipated thicknesses of the main boundary layer in air (0.30 inches) provided a design criterion for locating the side walls. If the thickness of the side wall boundary layer is taken to be of the same order of magnitude as the thickness of the main flow, six inches between the walls would seem sufficient to remove side wall effects.

Experimentally, these effects may be revealed by a temperature traverse laterally at a fixed distance from the leading edge and above the horizontal surface. Such a traverse was made in both water and air with the probe thermocouple located at the furthest possible position from the leading edge (12 inches). The results of the experiment in water are given in figure 5.1, where $c = 0.34\,^{\circ}F/ft.\ sec.$, for various times. It is noticed that a boundary layer formed near the edges but it did not seem to affect the central region (about 4 inches in width). During the preliminary tests, the tank was found to be inadequately sealed at the base, hence it was necessary to spread silicone rubber cement around the edges. As a result, this would account for the large region of influence at the side walls. The test in air revealed a similar temperature traverse.

5.2 LEADING EDGE EFFECTS

Linearization of the flow equations was possible by considering a horizontal surface of infinite extent, a condition which completely neglects leading edge effects. It is therefore doubtful if the linearized theory applies at a point in the system where leading edge effects occur for at such a point the effects of inertia and advection may be significant. Simulation of the infinite condition would

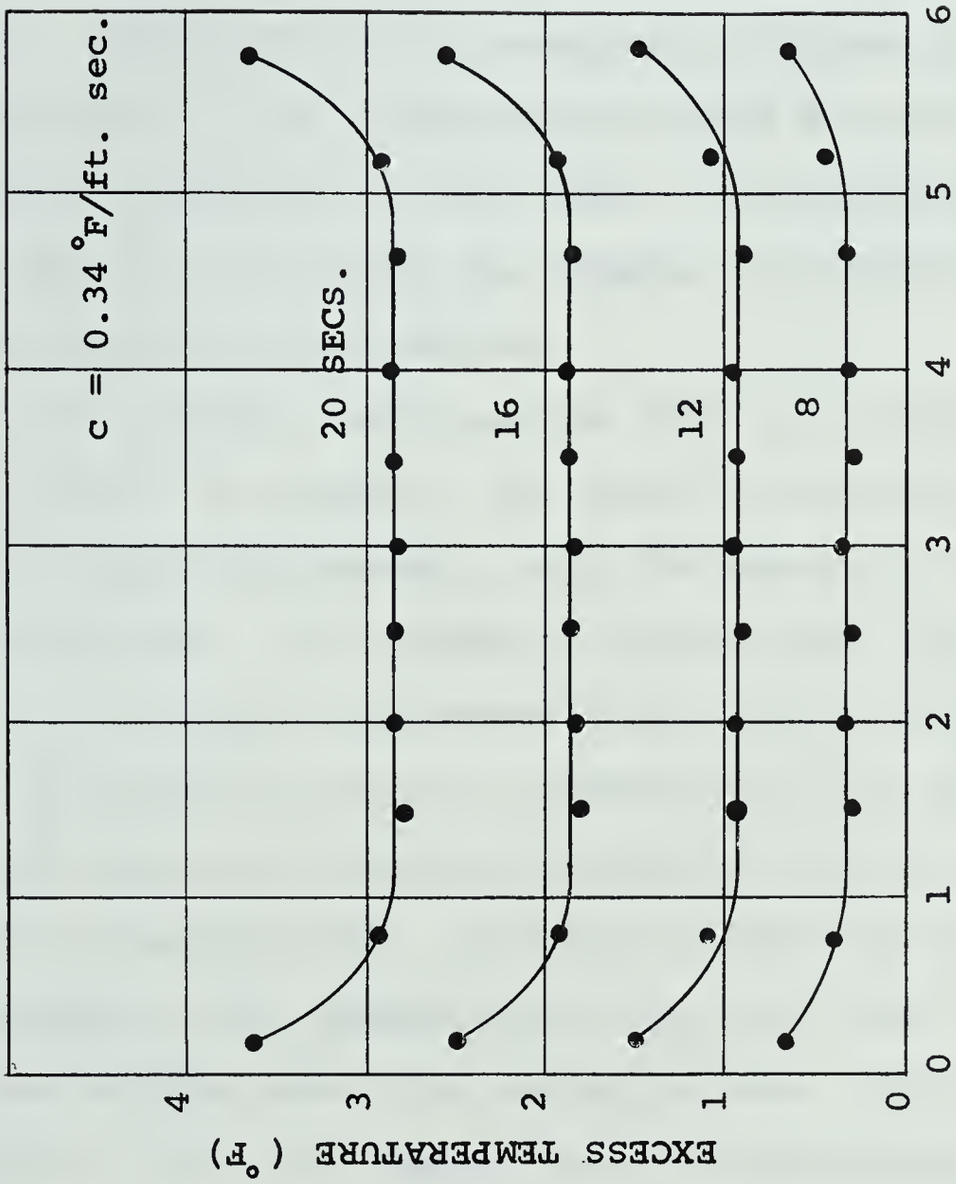

FIG. 5.1 LATERAL TEMPERATURE TRAVERSE

entail the use of an impractical apparatus, hence a finite plate (14 inches long) was used in combination with a detection method for predicting the onset of a leading edge effect. Preliminary runs revealed a distinct change in the behavior of the thermocouple output from the strip chart record of temperature versus time. Consequently, the time taken before this change was adopted for predicting the onset of leading edge effects.

The lengths of test periods differ considerably in water (about 20 seconds), air (about 12 seconds) and glycerine (about 60 seconds): only the tests in water are discussed here. By choosing a station about two-thirds of the test length downstream of the leading edge it was found possible to obtain a sufficiently long test period and yet avoid any possible disturbance caused by backwash from the trailing edge. A survey of the time taken before the change in the thermocouple output was then made for various heights above the heated surface. This is shown in Table I for three tests. As would be expected, it is

DISTANCE FROM SURFACE (INS)	PERIOD OF "ONE-DIMENSIONAL" BEHAVIOR (SECS)		
	c = 0.27	c = 0.34	c = 0.49
0.010	25	21	20
0.020	23	18	16
0.035	23	18	15
0.055	23	18	16
0.095	24	20	19

TABLE I ONSET OF LEADING EDGE EFFECT

evident that the time decreases as the rate of change of surface temperature gradient (c) increases. Also noticeable is a definite minimum with respect to height for each series. This is consistent with the shape of the velocity profile which might suggest a minimum leading edge free period near the velocity maximum. In view of the absence of a sharply pronounced minimum it appears that the onset of the leading edge effect could be estimated quite accurately from the bulk velocity.

5.3 DIRECT EFFECT OF GRAVITY

For laminar natural convection flow on a vertical plate the generating body force acts parallel to the plate whereas on a horizontal surface it acts normal to plate. In the latter case the body force still generates the flow but only indirectly. On an inclined plate, components acting both parallel and normal to the plate would each govern the flow behavior but for small angles from the horizontal little effect due to the former might be expected.

A series of tests were made in water by holding c constant and then recording temperature profiles for various plate angles. The results are given in figure 5.2a for downward inclinations and in figure 5.2b for upward inclinations, where both inclinations are relative to the leading

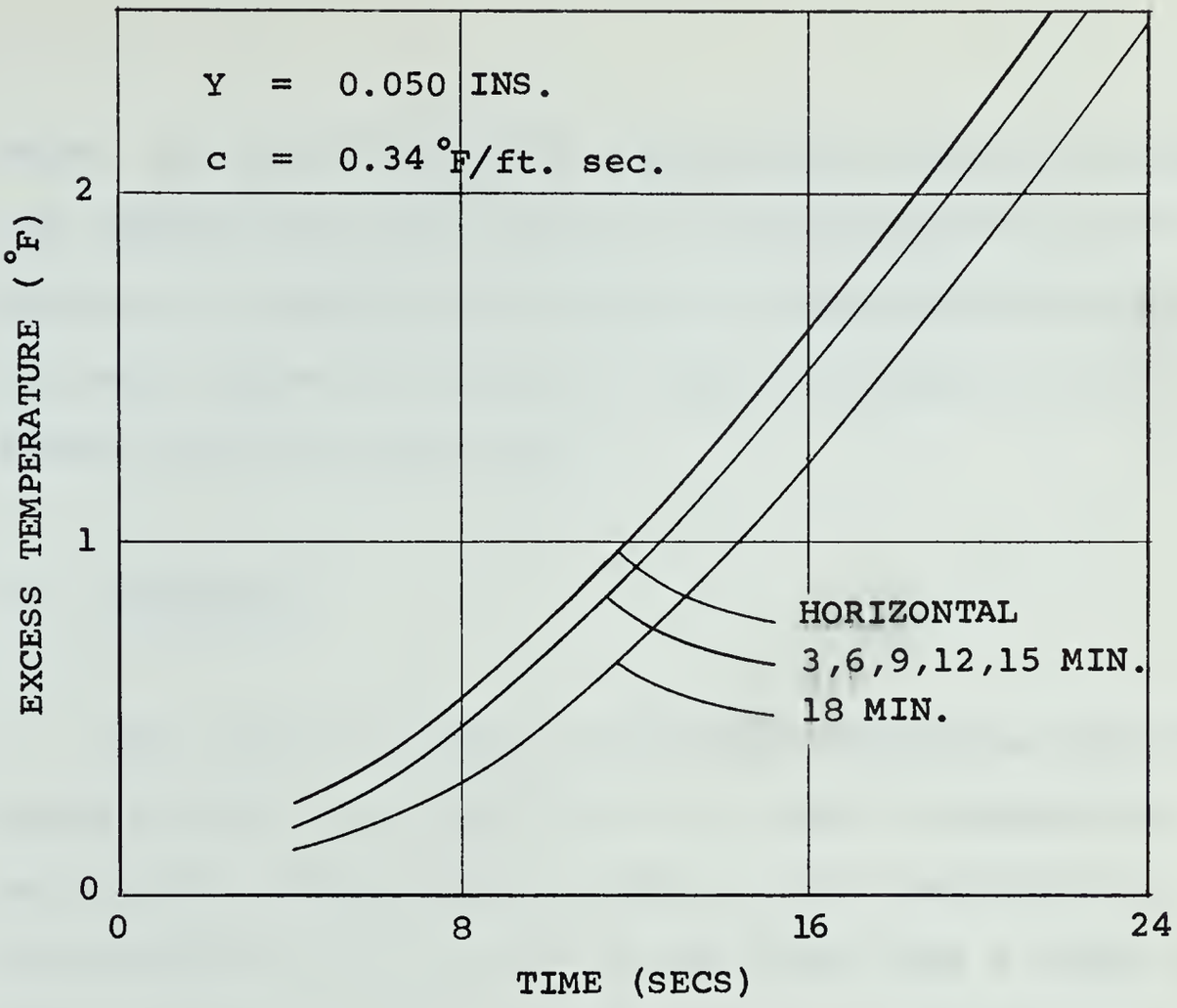

(a) INCLINED DOWN

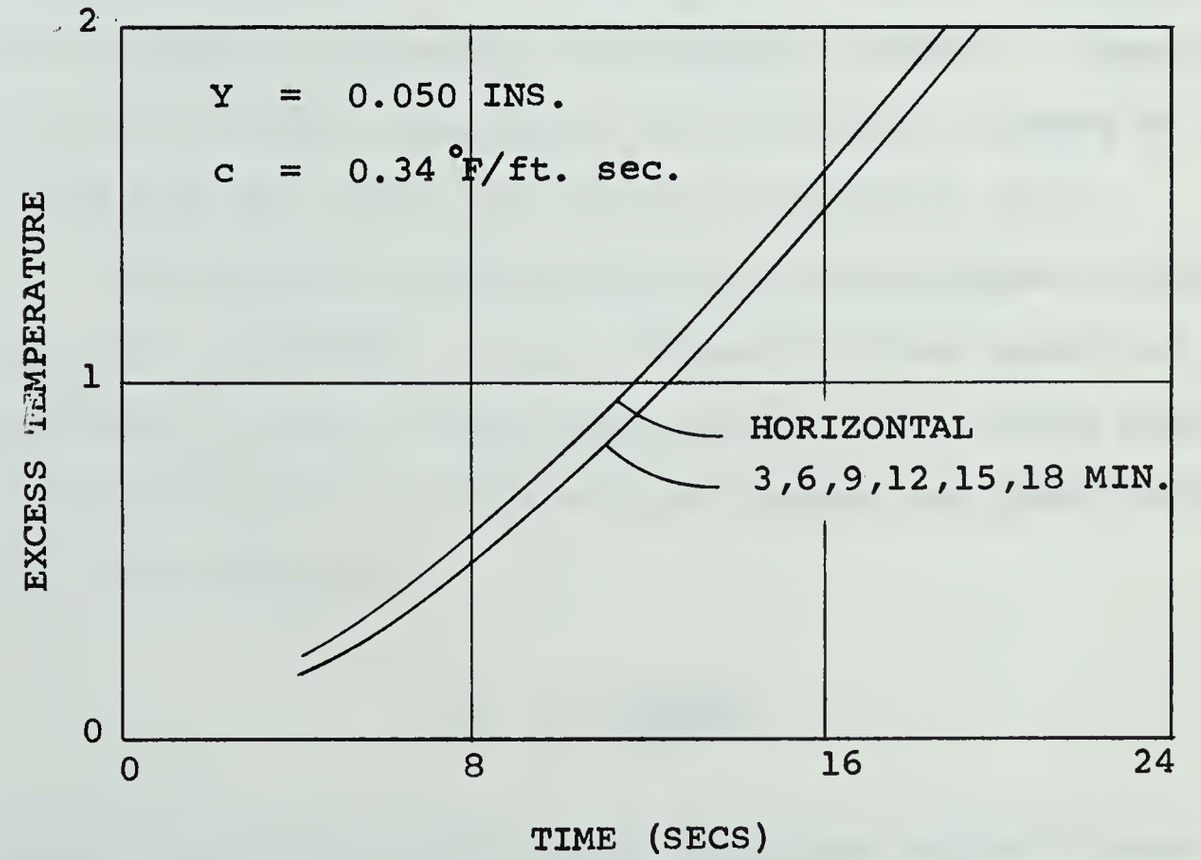

(b) INCLINED UP

FIG. 5.2 VARIATION OF TEMPERATURE WITH INCLINATION

edge. In view of possible experimental errors in recording temperatures and time and an uncertainty of $\pm$ 0.25 minutes in inclination, it may be concluded that no significant change was observed within an angle of $\pm$ 15 minutes from the horizontal.

5.4 STABILITY

Two layers of fluid of different densities with the heavier above the lighter are in a state of metastable equilibrium. Extensive studies (3) have been made on a meteorological scale where it was found that a layer of fluid heated from below would become unstable depending on a critical parameter (the Rayleigh number). Superposition of a steady flow along the horizontal surface in contrast has the effect of promoting stability (17).

The Rayleigh number associated with thermal instability in a quiescent layer of fluid for free upper and lower surfaces, or for a free upper surface and a rigid lower surface and for the case of rigid upper and lower surfaces has been defined as

$$Ra = \frac{\beta g h^3 \Delta\theta}{k\nu} ,$$

where h is the boundary layer thickness and $\Delta\theta$ is the temperature difference between the two surfaces. Choosing

$\Delta\theta$ as the excess temperature near the probe thermocouple, the Rayleigh number was calculated at the end point of each test discussed in Chapter 4. Table II summarizes the results. The critical Rayleigh number for a free isothermal upper surface and a rigid isothermal lower surface is about 1100(18), hence Table II suggests that only one water test (c = 0.49 °F/ft. sec.) may have been incipiently unstable. This seems to be in agreement with an observed temperature oscillation near the end point of that test.

Glycerine	c = 0.49	Ra = 11
Air	0.52	20
Water	0.27	960
Water	0.34	1300
Water	0.49	1700

TABLE II FINAL RAYLEIGH NUMBERS

5.5 MISCELLANEOUS OBSERVATIONS

Observation on finite suspended particles in the water tests indicated the existence of a region where viscous effects dominate near the horizontal surface. From these observations it was possible to estimate the bulk velocity, about 2 cm./sec., for c = 0.34 °F/ft. sec. By a similar

technique in glycerine, (with a dye streak in the lateral direction) flow was also observed resulting in an estimated bulk velocity of ($c = 0.52\,^{\circ}F/ft.\ sec.$) about 0.25 cm./sec. In view of the thin boundary layer thicknesses, quantitative measurements by these techniques were not possible.

Another aspect which might have influenced experimental results appreciably was the formation of air bubbles in water on all surfaces. These were noted to be of the order of the thermocouple diameter (0.010 inches). To overcome this problem, each time new tap water was used it was heated slightly and then allowed to de-aerate over a twenty-four hour period hence eliminating all observable entrained air.

A final aspect which may have influenced the experimental results is the possibility of "back flow" depending on the depth of fluid. To determine the effect of depth of fluid on the temperature distribution, profiles were recorded for various depths of water with the probe thermocouple located at 0.030 inches from the surface and seven inches from the leading edge ($c = 0.32\,^{\circ}F/ft.\ sec.$). Figure 5.3 illustrates the results. It is noticed that thermal instability was not detected and in view of the insignificant disagreement the depth of fluid does not seem to influence temperature profiles.

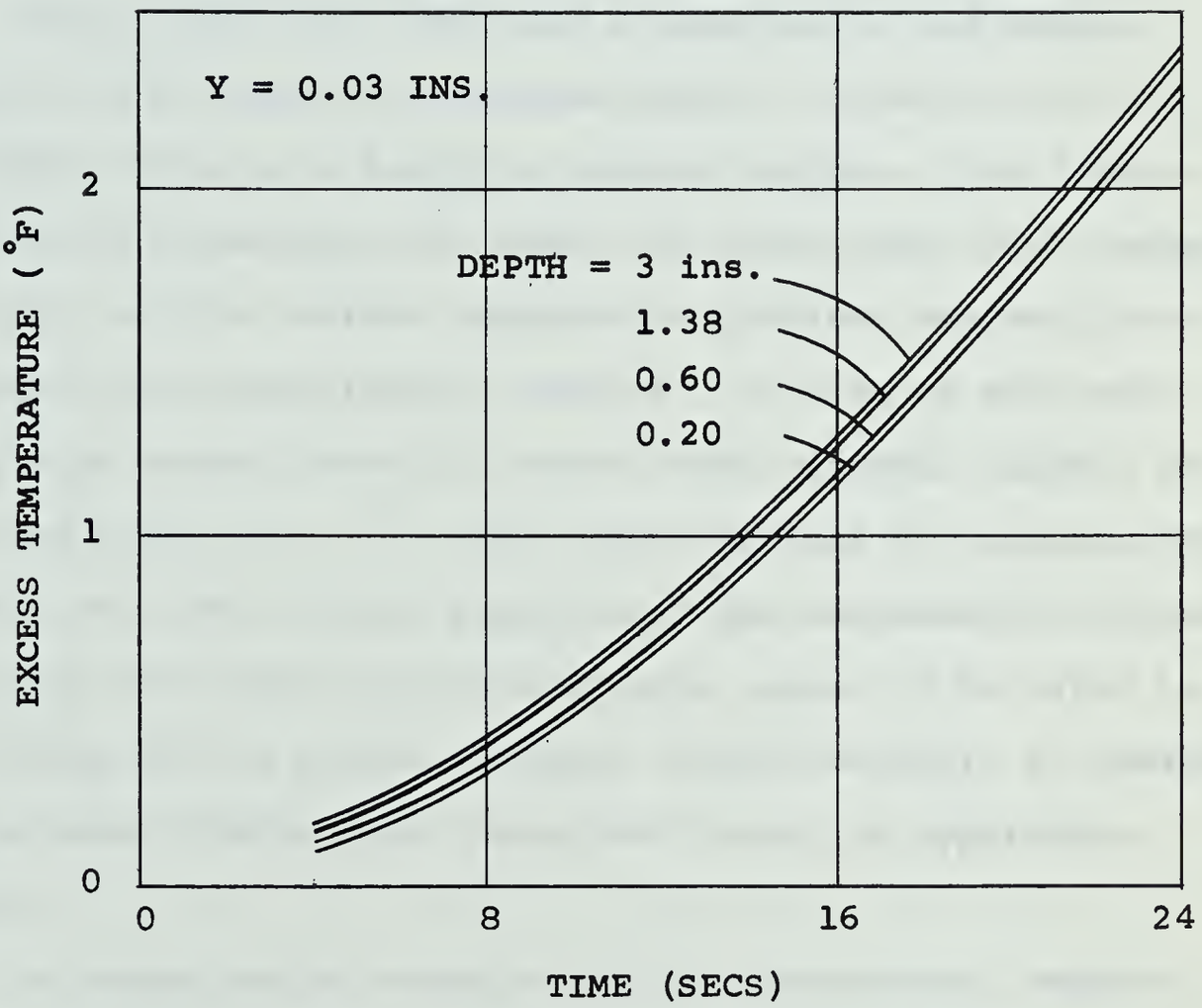

FIG. 5.3 VARIATION OF TEMPERATURE WITH TIME FOR VARIOUS DEPTHS OF WATER

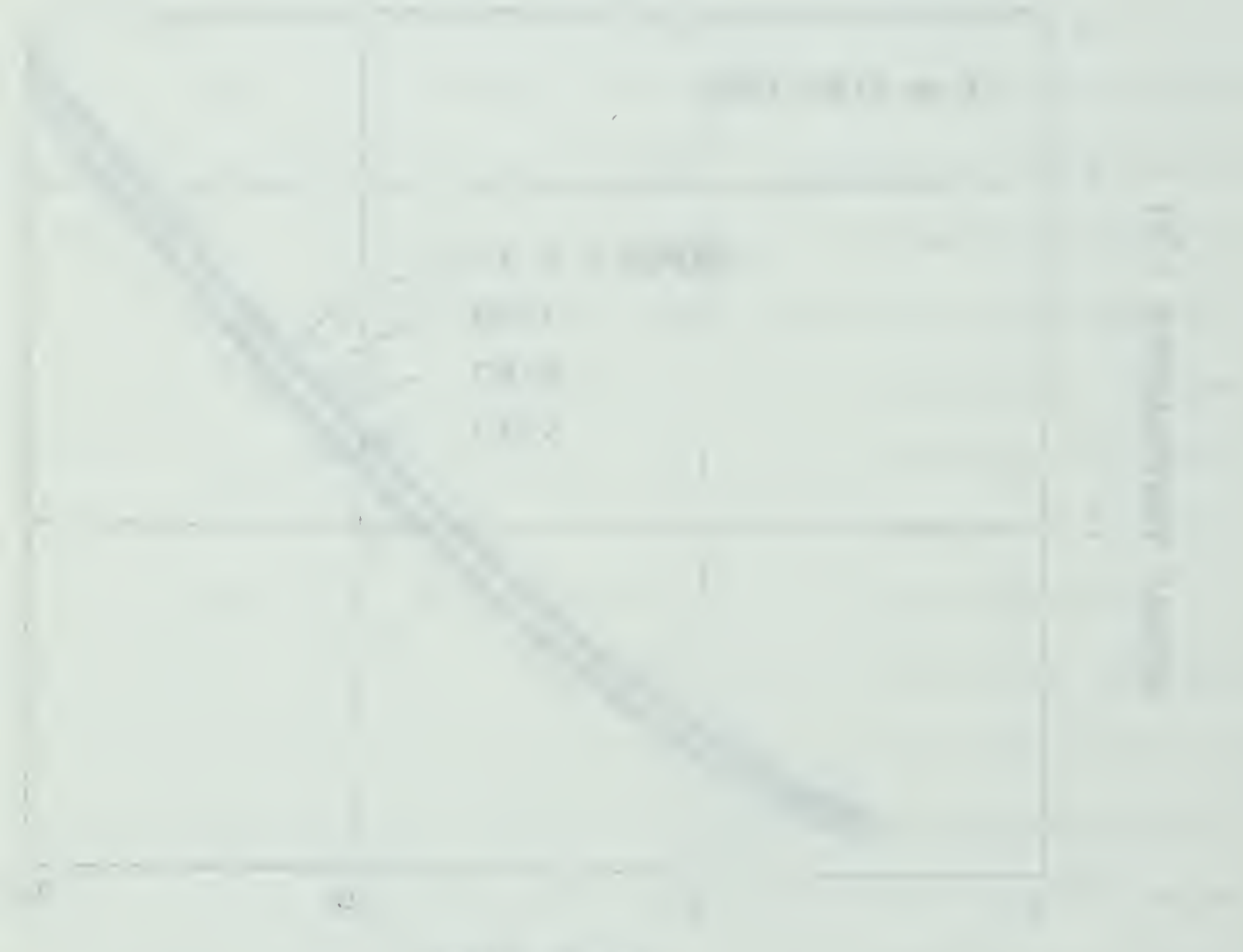

CHAPTER VI

CONCLUSIONS AND RECOMMENDATIONS

6.1 CONCLUSIONS

This thesis has described a theoretical and experimental investigation of laminar natural convection in the unsteady state on a large horizontal surface. The linearized theory developed for power law variations (with respect to time) of the surface temperature gradient was well supported by the experimental results. In view of the range of fluids tested, that is, those within Prandtl numbers of 3.0 and about 12×10^3, this indicates that the inertia and advection terms are not significant for non-metallic liquids. Although the theoretical predictions appear to be valid in the range of low Prandtl numbers (liquid metals), it remains to be shown whether the linearized theory is applicable there.

A comparison of experimental and theoretical temperature profiles for water revealed good overall agreement. Discrepancies, although never large, appear to be greatest near the region of the velocity maximum and this is consistent with the possible effect of inertia as felt through the velocity maximum. A similar comparison for tests in glycerine also revealed good overall agreement with no large deviations in any region of the velocity profile. This is

consistent with the expected dominance of viscosity at large Prandtl numbers. An experiment performed in air was not in good agreement with the linear theory. In view of a consistent disagreement, radiation losses seem to be significant.

Differences, between the temperature profiles obtained for various angles of the plate from the horizontal and the temperature profiles obtained at the horizontal position, were found to be insignificant in the range of plus or minus fifteen minutes of slope. Tests performed in water under various depths of fluid revealed a negligible difference in the temperature profiles for depths of fluid less than three inches. Existence of flow was demonstrated by observing small particles suspended in water and a dye streak in glycerine.

The results, and hence the conclusions, are only valid for circumstances in which the effect of a leading edge can be ignored, in which the side edges are sufficiently far removed and only under moderate temperate changes.

In view of the consistent overall agreement, the linearized theory would be expected to accurately predict the gross characteristics of the boundary layer, particularly the heat transfer relations.

6.2 APPLICATIONS

Although only the heated plate facing upwards has been studied in this thesis, a slight alteration will result in similar expressions for a heated plate facing downwards. Cooled plates either facing up or down may also be analyzed on the same basis; only the boundary conditions on the surface temperature gradient are altered.

Applications of these "gravity" flows are most likely realized on a micrometeorological or oceanographic scale; in particular in the study of ocean currents or sea breezes. These problems are more difficult than the present developed linearized theory would suggest, but it might be used as a zeroth approximation. In the field of civil engineering, it might be used in the study of density currents in resevoirs and lakes where the mass transfer problem is analogous to the heat transfer problem.

6.3 RECOMMENDATIONS

Conclusions regarding the effects of inertia and advection have been reported from experimental temperature profiles only. A more appropriate method would be a direct study of the experimental velocity profile. Complexity due to small velocities in the unsteady state makes it impossible at the present time to devise a direct velocity

measuring instrument. It may be feasible to use a fibre anemometer but current steady state devices are impractical for unsteady state conditions. Indications of bulk velocities are attainable by observing suspended particles in water and also by timing the movement of a dye streak in glycerine between two points on the horizontal surface.

To justify the validity of the approximations in the linearized theory over the full range of Prandtl number, the experimental work should be extended to the liquid metals. This would involve the re-designing of a larger tank, since times for the propagation of leading edge effects are much shorter. Further, the solutions should be extended to include the non-linear terms for these might become significant at low Prandtl numbers.

Laying thermocouples beneath the surface was found to be impractical (malfunction due to differential expansion) whereas, thermocouples placed on top of the surface worked well. In view of the linear temperature gradient near the wall, the actual surface temperature was obtained by linear extrapolation.

REFERENCES

1. LORD RAYLEIGH, "On Convection Currents in a Horizontal Layer of Fluid, when the Higher Temperature is on the Under Side", Philosophical Magazine, Series 6, vol. 32 (1916), p. 529.

2. BENARD, H., "Tourbillions Cellulaires dan une Nappe Liquide", Revue générale des Sciences pures et appliquées, vol. 11 (1900), p. 1261 and p. 1309.

3. OSTRACH, S., "Convection Phenomena in Fluids Heated from Below", ASME Transactions, vol. 79 (1957), p. 299.

4. STEWARTSON, K., "On the Free Convection from a Horizontal Plate", Journal of Applied Mathematics and Physics (ZAMP), vol 1Xa (1958), p. 276.

5. LEVY, S., "Integral Methods in Natural Convection Flow", Journal of Applied Mechanics (ASME), vol. 22, No. 4 (1955), p. 515.

6. SUGAWARA, S. and MICHIYOCHI, I., "Heat Transfer from a Horizontal Flat Plate by Natural Convection", Transactions of the Japanese Society of Mechanical Engineers (JSME) vol. 21, No. 109 (1955), p. 651.

7. WEISE, R., "Warmeübergang durch freie Konvektion an quadratischen Platten", Forshung auf dem Gebiete des Ingenieurwesens, vol. 6 (1935), p. 281.

8. JEFFREYS, H., "On the Dynamics of Wind", Quarterly Journal of the Royal Meteorological Society, vol. 48 (1922), p. 29.

9. PEARCE, R.P., "A Simplified Theory of the Generation of Sea Breezes", Quarterly Journal of the Royal Meteorological Society, vol. 88 (1962), p. 20.

10. ESTOQUE, M.A., "A Theoretical Investigation of the Sea Breeze", Quarterly Journal of the Royal Meteorological Society, vol. 87 (1961), p. 136.

11. FISHER, E.L., "A Theoretical Study of the Sea Breeze", Journal of Meteorology, vol. 18 (1961), p. 216.

12. FISHER, E.L., "An Observational Study of the Sea Breeze", Journal of Meteorology, vol. 17 (1960), p. 645.

13. SPARROW, W.M. and GREGG, J.L., "The Variable Fluid - Property Problem In Free Convection", ASME Transactions, vol. 80 (1958), p. 879.

14. HELLUMS, J.D. and CHURCHILL, S.W., "Dimensional Analysis and Natural Circulation", Chemical Engineering Progress Syposium, Series No. 32, vol. 57, p. 75.

15. NORDON, J., "Sur une solution nouvelle de l'équation de Fourier", Acad. Sci. Paris, Comptes Rendus, vol. 228, (1949), p. 167.

16. RICH, R.B., "An Investigation of Heat Transfer from an Inclined Flat Plate in Free Convection", ASME Transactions, vol. 75 (1953), p. 489.

17. JEFFREYS, H., "Some Cases of Instability in Fluid Motion", Proceedings of the Royal Society, Series A, vol. 118, (1928).

18. SPARROW, E.M., GOLDSTEIN, R.J. and JONSON, V.K., "Thermal Instability in a Horizontal Fluid Layer", Journal of Fluid Mechanics, vol. 18, Part 4 (1964), p. 513.

19. KREITH, K., "Principles of Heat Transfer", sixth printing (1962), International Textbook Company, Scranton.

20. KAYE, J., "A Table of the First Eleven Repeated Integrals of the Error Functions", Journal of Mathematics and Physics, vol. 34 (1955), p. 119.

APPENDIX A

VALIDITY OF APPROXIMATIONS

Consider the validity of the approximations made in Chapter II for a test in water ($c = 0.34\,^{\circ}F/ft.sec.$).

First examine the orders of magnitude of the combined momentum equation

$$\frac{\partial^2 u}{\partial y \partial \tau} = \frac{\partial^3 u}{\partial y^3} - \frac{\partial \phi}{\partial x} \quad . \qquad \text{A-1}$$

If the problem is to be properly posed both the unsteady and "driving" term must remain. It therefore remains to be shown that the viscous term is of the same order of magnitude.

Given $X = 1.25$ ft., $Y = 0.0084$ ft., $U = 0.065$ ft/sec.,

$X_o = Y_o = 0.0095$ ft., $U_o = 0.0011$ ft/sec.,

and $t_o = 9.0$ sec.,

a substitution into A-1 leads to

$$600/t = 85 - 0.26\,\theta_X \quad ,$$

noting that the value of U was obtained as mentioned in Chapter V, section 5.5. Examining the relative orders of magnitude, it seems reasonable that each term in A-1 is of the same order.

Now consider approximations of

$$\frac{\partial \phi}{\partial \tau} + u \frac{\partial \phi}{\partial x} = \frac{1}{\sigma}\left(\frac{\partial^2 \phi}{\partial y^2}\right) \qquad \text{A-2}$$

Given σ to be about 5.9, a substitution into A-2 gives

$$\left[310/t + 16 = 8\right] \Delta\theta \quad , \qquad \text{A-3}$$

where $\Delta\theta$ has been taken outside the bracket since it is a common factor when A-2 is written in terms of finite difference quotients. Examining A-3 it appears that advection may not be neglected but since Chapter II considers an infinite plate and since x may be any value without changing the other two terms, it seems justified to neglect advection.

Consider the validity of neglecting dissipation, namely

$$0 \leq \left[2\left(\frac{\partial u}{\partial x}\right)^2 + \left(\frac{\partial v}{\partial y}\right)^2 + \left(\frac{\partial u}{\partial y}\right)^2 + \left(\frac{\partial v}{\partial x}\right)^2 + 2\left(\frac{\partial u}{\partial y}\ \frac{\partial v}{\partial x}\right)\right] .$$

$(\partial u/\partial y)^2$ is the only large term in the bracket, therefore the magnitude of the dissipation term is

$$5 \times 10^{-7} \times 67 .$$

As a result, it seems justified to neglect dissipation when compared to A-3. It is important to note that near the critical point of a fluid where β becomes large dissipation may not be neglected.

APPENDIX B

SOLUTIONS BY LAPLACE TRANSFORMS

Consider a solution of the conduction equation

$$\frac{\partial \phi}{\partial \tau} = \frac{1}{\sigma}\left(\frac{\partial^2 \phi}{\partial y^2}\right) \qquad \text{B-1}$$

with boundary conditions $\phi(o) = x\tau^n$, $\phi(\infty) = 0$. The Laplace transform of equation B-1 with respect to the variable τ is

$$s\bar{\phi} = \frac{1}{\sigma}\frac{d^2\bar{\phi}}{dy^2},$$

with boundary conditions $\bar{\phi}(o,s) = \frac{x\Gamma(n+1)}{s^{n+1}}$, $\bar{\phi}(\infty,s) = 0$ where $n > -1$.

Solving,

$$\bar{\phi} = \frac{x\Gamma(n+1)}{s^{n+1}} e^{-\sqrt{\sigma s}\, y}$$

the inverse of which is

$$\phi = x\tau^n 2^{2n} \Gamma(n+1)\, i^{2n} \operatorname{erfc}\left[y/\left(\frac{4\tau}{\sigma}\right)^{1/2}\right] \qquad \text{B-2}$$

where $2n = 0,1,2, \ldots\ldots$.

Hence, substituting B-2 into the y-momentum equation 2.1-9, integrating, and satisfying the condition on pressure at infinity gives

$$p = -x\tau^{n}\left(\frac{4\tau}{\sigma}\right)^{1/2} 2^{2n}\,\Gamma(n+1)\; i^{2n+1}\,\mathrm{erfc}\left[y/\left(\frac{4\tau}{\sigma}\right)^{1/2}\right]. \qquad \text{B-3}$$

To determine the velocity distribution, consider a solution of the x-momentum equation

$$\frac{\partial u}{\partial \tau} = -\frac{\partial p}{\partial x} + \frac{\partial^2 u}{\partial y^2} \qquad \text{B-4}$$

consistent with $u(o) = u(\infty) = 0$.

Upon substitution of B-3 into B-4, the Laplace transform of B-4 with respect to τ using the initial condition $u(x,y)_{\tau=0} = 0$ yields

$$s\bar{u} = \frac{d^2\bar{u}}{dy^2} - \frac{\Gamma(n+1)}{\sigma^{1/2}}\,\frac{e^{-\sqrt{\sigma s}\,y}}{s^{n+3/2}} \qquad \text{B-5}$$

with $\bar{u}(o,s) = \bar{u}(\infty,s) = 0$.

By inspection B-5 has a particular integral given by

$$\bar{u}_p \propto \frac{\Gamma(n+1)}{\sigma^{1/2}}\,\frac{e^{-\sqrt{\sigma s}\,y}}{s^{n+3/2}} \;;$$

substituting into B-5 results in

$$\bar{u}_p = \frac{\Gamma(n+1)}{(1-\sigma)\,\sigma^{1/2}}\,\frac{e^{-\sqrt{\sigma s}\,y}}{s^{n+5/2}} \;.$$

Seeking the complete solution in the form

$$\bar{u} = Ae^{\sqrt{s}\,y} + Be^{-\sqrt{s}\,y} + \frac{\Gamma(n+1)}{(1-\sigma)\sigma^{1/2}} \frac{e^{-\sqrt{\sigma s}\,y}}{s^{n+5/2}}, \qquad B\text{-}6$$

$\bar{u}(\infty,s) = 0$ requires that $A = 0$ and

$\bar{u}(o,s) = 0$ requires

$$B = \frac{\Gamma(n+1)}{(1-\sigma)\sigma^{1/2}\, s^{n+5/2}} .$$

Hence, the inverse of B-6 becomes

$$u = \frac{\Gamma(n+1)}{(1-\sigma)\sigma^{1/2}} (4\tau)^{n+3/2}\left[i^{2n+3}\ \mathrm{erfc}\ y/\left(\frac{4\tau}{\sigma}\right)^{1/2} - i^{2n+3}\ \mathrm{erfc}\ y/\left(4\tau\right)^{1/2}\right]$$

which agrees with the expression 2.2-10.

APPENDIX C

INFLUENCE OF LATERAL VELOCITIES

If the Teflon plate were inclined laterally, a component of velocity in this direction would be possible. The purpose of this appendix is to determine the order of magnitude of this component hence permitting a comparison to be made with the velocity of the main flow.

Consider the inclined isothermal plate of figure C.1 consistent with the boundary conditions,

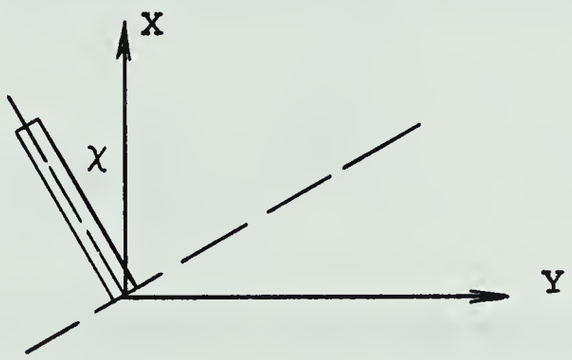

FIG. C-1 COORDINATE SYSTEM

$$\theta(o) - Bt = U(o) = 0$$

$$\theta(\infty) = U(\infty) = P_d(\infty) = 0.$$

Applying the same approximations as in Chapter II, the governing boundary layer equations become:

$$\frac{\partial U}{\partial X} + \frac{\partial V}{\partial Y} = 0$$

$$\frac{\partial U}{\partial t} = -\frac{1}{\rho} \frac{\partial P_d}{\partial X} + \beta g \theta (\cos \chi) + \nu \frac{\partial^2 U}{\partial Y^2}$$

$$0 = \beta g \theta (\sin \chi) - \frac{1}{\rho} \frac{\partial P_d}{\partial Y}$$

$$\frac{\partial \theta}{\partial t} = \kappa \frac{\partial^2 \theta}{\partial Y^2}$$

Considering a solution of the energy equation, the Laplace transform with respect to the variable t is

$$s\bar{\theta} = \kappa \frac{d^2\bar{\theta}}{dY^2} ,$$

with boundary conditions $\bar{\theta}(o,s) = \frac{B}{s^2}$ and $\bar{\theta}(\infty,s) = 0$.

Solving,

$$\bar{\theta} = \frac{B}{s^2} e^{-\sqrt{\frac{s}{\kappa}} Y} ,$$

the inverse of which results in the temperature distribution

$$\bar{\theta} = B(4t)\, i^2 \operatorname{erfc} \frac{Y}{2\sqrt{\kappa t}} . \qquad \text{C-1}$$

Hence, by substituting C-1 into the Y-momentum equation, integrating, and satisfying the boundary condition on pressure at infinity gives

$$P_d = -B(\sin \chi)\, \beta g \rho (8t)(\kappa t)^{1/2}\, i^3 \operatorname{erfc} \frac{Y}{2\sqrt{\kappa t}} \qquad \text{C-2}$$

It is noticed that the pressure does not vary with X (i.e.

there is no variation of the departure of pressure from hydrostatic conditions in the lateral direction at a given time).

The velocity distribution may now be obtained from the X-momentum equation by firstly substituting C-1 and C-2, resulting in

$$\frac{\partial U}{\partial t} = (\cos \chi)\, \beta B g (4t)\, i^2\, \mathrm{erfc}\, \frac{Y}{2\sqrt{\kappa t}} + \nu \frac{\partial^2 U}{\partial Y^2} . \qquad C\text{-}3$$

The Laplace transform of C-3 with respect to t after applying the initial condition $U(X,Y)_{t=0} = 0$ yields

$$s\bar{U} = \nu \frac{d^2\bar{U}}{dY^2} + \frac{B\beta g (\cos \chi)\, e^{-\sqrt{\frac{s}{\kappa}}\, Y}}{s^2} , \qquad C\text{-}4$$

the solution of which must be consistent with

$$\bar{U}(o,s) = \bar{U}(\infty,s) = 0.$$

Assuming the particular integral of C-4 is of the form

$$\bar{U}_p \propto \frac{\beta g B (\cos \chi)\, e^{-\sqrt{\frac{s}{\kappa}}\, Y}}{\nu \quad s^2} ,$$

substitution gives,

$$\bar{U}_p = \frac{\beta g B (\cos \chi)}{(1-\sigma)} \quad \frac{e^{-\sqrt{\frac{s}{\kappa}}\, Y}}{s^3} .$$

Hence, seeking the total solution in the form

$$\bar{U} = Ae^{\sqrt{\frac{s}{\kappa}}\,Y} + Ee^{-\sqrt{\frac{s}{\nu}}\,Y} + \frac{\beta g B(\cos\chi)}{(1-\sigma)}\,\frac{e^{-\sqrt{\frac{s}{\kappa}}\,Y}}{s^3}\,, \qquad \text{C-5}$$

$$\bar{U}(\infty, s) = 0 \text{ requires that } A = 0 \text{ and}$$

$$\bar{U}(o, s) = 0 \text{ requires}$$

$$E = \frac{-\beta g B(\cos\chi)}{(1-\sigma)\ s^3}\,.$$

Upon substitution for the coefficients, the inverse of C-5 may be written as

$$U = \frac{\beta g B(\cos\chi)(4t)^2}{(1-\sigma)}\left[i^4\,\text{erfc}\,\frac{Y}{2\sqrt{\kappa t}} - i^4\,\text{erfc}\,\frac{Y}{2\sqrt{\kappa t}}\Big/\sqrt{\sigma}\right] \qquad \text{C-6}$$

Examining C-6 it is evident that this velocity becomes very small for values of χ approaching $\pi/2$ and in comparison to the velocity of the main flow, namely

$$U = \frac{\beta g c\ \kappa\ (4t)^{5/2}}{(1-\sigma)}\left[i^5\,\text{erfc}\,\frac{Y}{2\sqrt{\kappa t}} - i^5\,\text{erfc}\,\frac{Y}{2\sqrt{\kappa t}}\Big/\sqrt{\sigma}\right],$$

it may be neglected. Hence, it would seem reasonable that the inaccuracy of the level of the plate transversely is not a major influencing factor.

APPENDIX D

DATA REDUCTION

Considering a test in water (as given in figures 4.1, 4.2, and 4.3) a typical procedure used in reducing the experimental data is as follows:

Firstly, all strip chart recordings were converted to temperature versus time curves by using figure D.1. Because of the linear nature of the temperature distribution close to the surface (see figure 2.2), it was possible to determine the actual surface temperature at any time by extrapolation on the temperature versus position (i.e. with respect to the surface) curves. Plotting this surface temperature distribution on the temperature versus time graph and extending it back to the abscissa, permitted a temporal origin to be defined. A typical re-plot with respect to this origin is then as given in figure 4.1. Since the probe was located at X = 12 $\pm$ 1/8 inches, c was found to be 0.34 $^{\circ}$F/ft.sec. from the slope of the surface temperature distribution. Hence knowing c, the pertinent theoretical curves could be obtained but not before converting

$$\theta = cX_o t_o \phi \quad \text{and} \quad \phi = x\tau\Phi, \qquad (n=1)$$

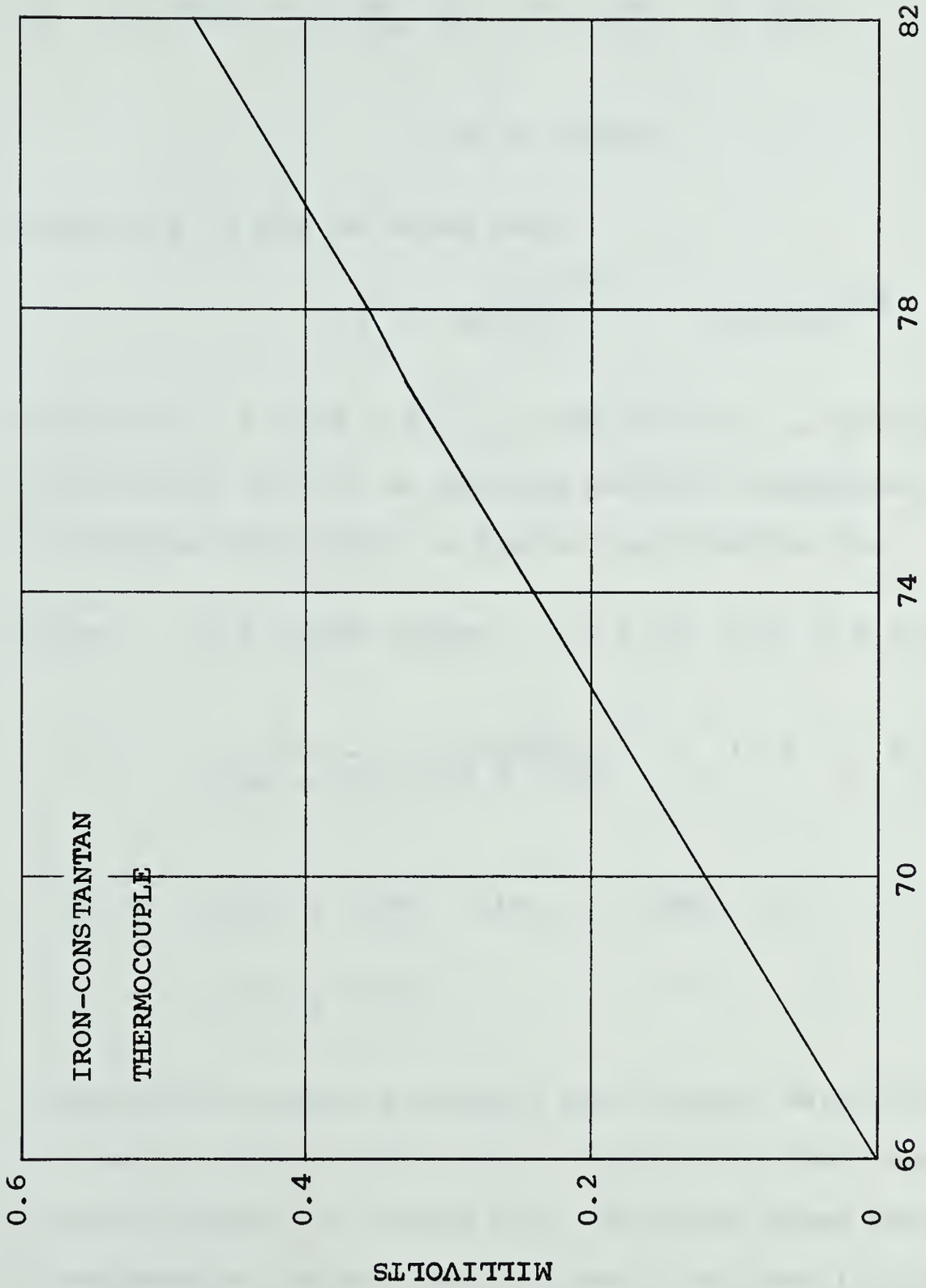

FIG. D.1 THERMOCOUPLE CONVERSION CHART

by utilizing $X = xX_o$ and $Y = yY_o$, to give

$$\theta = cXt\Phi.$$

Similarly it may be shown that

$$\eta = y/\left(\frac{4\tau}{\sigma}\right)^{1/2} = Y/2(\kappa t)^{1/2} .$$

Selecting $\kappa = 1.56 \times 10^{-6} \pm 2.0\%$ ft^2/sec. as obtained from tables (19) at an average surface temperature and using tables for Φ (20), a typical calculation is:

Given $Y = 0.045$ inches, $\eta = 0.40$ and $\Phi = 0.37$,

$$t = \frac{1}{1.56 \times 10^{-6}} \left(\frac{0.045}{24 \times 0.40}\right)^2 = 14.1 \pm 2.0\% \text{ sec.}$$

$$\theta = 0.34(1 \pm 1.0\%) \quad (14.1 \pm 2.0\%) \; 0.37$$

$$= 1.79\,^{\circ}\text{F} \pm 3.0\%.$$

Repeating the above procedure for several values of η at the same Y and then for all Y, results in the theoretical curves as given on figure 4.1. Plotting these curves on a temperature versus position basis resulted in figure 4.2.

All experimental points were then cross plotted from figures 4.1 and 4.2 to give the non-dimensional temperature profile of figure 4.3. Since overall errors are best

revealed on this type of curve, all experimental error calculations were restricted to this plot.

Considering a point in the maximum velocity region,

$$Y = 0.045" \pm 0.001$$
$$t = 12 \text{ sec} \pm 0.25$$
$$X = 1 \text{ ft.} \pm 0.01$$
$$\theta = 1.6\,^{\circ}F \pm 0.1 \quad ,$$

$$\Phi = \frac{\theta}{cXt} = 0.39 \pm 9.0\%$$

$$\eta = \frac{Y}{2\sqrt{\kappa t}} = 0.44 \pm 3.0\% \ .$$

These percentage errors were calculated for a number of points in the region near the surface, in the velocity maximum region, and also near the edge of the boundary layer. The maximum errors in each region are given in the main text of Chapter IV.